의학 박사 학위논문

동일 환자 유래 원발 대장암과 복막 전이암의 exosomal miR-193a 와 let-7g가 암 전이에 미치는 영향

Exosomal miR-193a and let-7g accelerate cancer progression on primary colorectal cancer and paired peritoneal metastatic cancer.

2021년 2월

서울대학교 대학원

의과학과 의과학 전공

조 우 철

Exosomal miR-193a and let-7g accelerate cancer progression on primary colorectal cancer and paired peritoneal metastatic cancer.

By Woo-Cheol Cho

(Directed by Ja-Lok Ku, D.V.M., Ph.D.)

A Thesis Submitted to the Department of Biomedical Sciences in Partial Fulfilment of the Requirements for the Degree of Doctor of Philosophy in Medicine (Biomedical Sciences) at Seoul National University College of Medicine

February, 2021

Approved by thesis committee

Professor Seung Tae Jeong Chairman

Professor Ja-Lok Ku Vice Chairman

Professor Sang-Kyu Ye

Professor Hang Rae Kim

Professor BYONG CHUL YOO

ABSTRACT

Colorectal cancer has the third highest incidence rate worldwide, and one of the various forms of colorectal cancer metastasis is metastasis to the peritoneum. A peritoneal metastasis of colorectal cancer is difficult to diagnose, and has a poor prognosis. Trans-mesothelial metastasis is a mechanism of peritoneal metastasis caused by contact with the peritoneum, and exosomes involved in cell-to-cell interaction are considered to play a crucial role in the cancer microenvironment and epithelial-mesenchymal transition. Therefore, this study tried to elucidate clinically the possibility of exosomal miRNA as diagnostic and prognostic marker. Exosomal miRNA was extracted and analyzed by miRNA microarray. The expression of exosomal miR-193a in the PTM group was lower than that of the primary CRC group, and the expression of exosomal let-7g was higher than that of the primary CRC. After selecting target genes of miR-193a and let-7g using the miRNA database, mRNA expression was confirmed for *MMP16* and *CDKN1A*. When the mimics of these two exosomal miRNAs were treated with cell

lines, both *MMP16* and *CDKN1A* (targets of miR−193a and let−7g) decreased intracellular expression. A cell invasiveness and proliferation assay were conducted to confirm the physiological role of the miR−193a and the let−7g. Cell invasiveness and proliferation were decreased by miR−193a and increased by let−7g. The differences in expression of exosomal miR−193a and let−7g extracted from the plasma of patients were classified as cancer progression indicators. Decreased miR−193a and increased let−7g were seen as cancer progression indicator. Furthermore, the survival rate decreased in the group with low miR−193a expression and high let−7g expression. This study elucidated the possibility of using this as a diagnostic and prognostic marker for colorectal cancer by measuring the expression levels of exosomal miR−193a and let−7g in blood.

Keywords: Colorectal cancer, Peritoneal metastasis, Exosome, miR−193a, let−7g

Student number : 2014−30668

TABLE OF CONTENTS

LIST OF TABLES

LIST OF FIGURES

Figure 6. Mutual and clinical correlation of exosomal miR−193a and let−7g expression (Kaplan−meier plot)

INTRODUCTION

Colorectal cancer (CRC) has the third highest incidence in the world among all cancer types, and it is estimated that 2.4 million will have occurred by 2035 (1). The peritoneum, one of the areas where colorectal cancer metastasizes and recurs, covers most of the organs in the abdomen, and supports many of these organs, holding them in position. This is where many nerves, blood vessels and lymphatic vessels pass. Therefore, the second most frequent occurrence of colorectal cancer recurrence or metastasis is known to be in the peritoneum because it has such close physical contact with other organs (2-4).

According to next generation sequencing analysis, only 10% of isolated metastases are in the peritoneum, but complex metastases in the liver and other organs, including the peritoneum, occurs more than 20% of the time (5).

The diagnosis of peritoneal metastasis through visualization such as CT or PET is difficult. Early diagnosis is likewise difficult because of the sporadic spread of the peritoneal cancer in a very

small and flat form. Peritoneal metastasis is often found only near the end stage (6). Therefore, peritoneal metastasis tends to be only relatively resistant to systemic therapy, but it also has poor prognosis (3,7-9).

There is a treatment that can be performed in patients with selective conditions at a high medical level and environment. Hyperthermic intraperitoneal chemotherapy (HIPEC) is performed simultaneously following cytoreductive surgery, which suppresses the progression of peritoneal metastasis (10-13). However, this treatment is known to have a high risk of mortality. Recently, HIPEC and second-look surgery treatments have been used in a preventive manner to control cancers at the early stages of progression (14-16).

Liquid biopsy through blood samples can be detected at an early stage of cancer, and simultaneous monitoring allows relatively quick and easy determination of anticancer drug resistance and the possibility of recurrence (17-19).

Recently, studies have been actively performed by extracting

exosomes in blood (20–22). Exosomes contain miRNAs and proteins as well as DNA. Specific miRNAs in exosomes can be used as markers for colon cancer recurrence (23–25). Several studies have reported that exosomes increase the tumor–like behavior of mesenchymal stem cells (26–29).

A miRNA is a short (20—24 nt) noncoding RNA that is involved in the post–transcriptional regulation of gene expression in multicellular organisms by affecting both the stability and the translation of mRNAs (27). Furthermore, miRNAs target protein–coding mRNAs at the posttranscriptional level by direct cleavage to the mRNAs or by inhibition of protein synthesis.

Recent studies indicate that exosomal miRNAs have been identified in plasma and are important as noninvasive liquid biomarkers for cancer patients (23,30,31).

Considering the convenience of exosomal miRNAs that can be extracted from patients by a liquid biopsy and the effect of changing the physiological role of colorectal cancer, this study attempted to elucidate exosomal miRNA markers for peritoneal metastatic

colorectal cancer, which is difficult to diagnose and has a poor prognosis, through miRNA microarray in primary and paired peritoneal metastasis cell lines. Furthermore, this study tried to confirm the significance of the expression of the miRNA markers in exosomal miRNAs extracted from the patient's blood. Furthermore, it is expected that these studies will be used as a basic study to reveal the significance of miRNA markers and progression of colon cancer patients.

MATERIALS AND METHODS

Cell culture

The cells used in this study were obtained from the Korean Cell Line Bank. All colorectal cancer and paired peritoneal metastatic cancer cell lines (SNU-2335A, SNU-2335D, SNU-2404A, SNU-2404B, SNU-2414A, SNU-2414B, KM12C, KM1214, SW480 and SW620) were routinely cultured in RPMI1640 media (Gibco; Thermo Fisher Scientific, Inc.) supplemented with 10% fetal bovine serum (FBS; Gibco; Thermo Fisher Scientific, Inc.), 100 U/mL penicillin and 100 μg/mL streptomycin (Gibco; Thermo Fisher Scientific, Inc.). All cell lines were cultured in a humidified incubator at 37°C containing 5% CO_2 and 95% air.

Human plasma samples

A total of 69 cases of plasma samples were collected from CRC patients before surgery in Seoul National University Hospital between May 29, 2014 and November 12, 2015. This study was conducted in accordance with the Declaration of Helsinki. Written

informed consent was obatained from each subject or each subject's guardian. All research were performed after approval by an institutional review board of Seoul National University Hospital (IRB no. 1103-125-357). Whole blood was collected through venipuncture, and whole blood was dispensed into an Eppendorf tube (E-tube) within 3 h. After 30 μL of protease inhibitor was added to each E-tube, it was centrifuged at 4°C, 1500 × g for 10 min. The supernatant was transferred to new tube and stored in a deep freezer (–80°C) until needed.

Exosome isolation

Cell culture medium. Exosome was isolated using total exosome isolation (from cell culture media) reagent (cat no.4478359, Thermo Fisher Scientific, Inc.). Cell culture medium was harvested and was centrifuged the cell medium at 2000 × g for 30 min. Supernatant was transferred to a new tube and mixed with exosome isolation reagent (culture medium: reagent = 2 : 1). Medium-reagent mixture was incubated at 4°C for overnight. After incubation, the mixture was centrifuged at 10000 × g for 1 h at 4°C. The mixture

pellet was resuspended in PBS.

Plasma. Exosome was isolated using total exosome isolation (from plasma) reagent (cat no.4484450, Thermo Fisher Scientific, Inc.). Plasma sample was centrifuged at 2000 × g for 30 min. The supernatant was transferred to new tube and centrifuged at 10000 × g for 20 min to romove debris. The clarified plasma was mixed with 0.5 volumes of PBS and 0.05 volumes of proteinase K was added to sample. Exosome precipitation reagent (0.2 volume) was added to mixture of plasma and PBS. The sample was incubated at 4°C for 30 min. After incubation, the sample was centrifuged at 10000 × g for 5 min at room temperature (RT). The supernatant of sample was aspirated and exosome pellet was resuspended by PBS.

Exosomal miRNA extraction

Exosomal miRNA was extracted by Total Exosome RNA & Protein Isolation Kit (cat no.4478545, Thermo Fisher Scientific, Inc.) according to the manufacturer's instructions. 200 μL of Suspended exosome in PBS was mixed with 200 μL of 2× denaturing solution (prewarmed at 37°C) and was incubated on ice for 5 min. 400 μL of

Acid-Phenol:Chloroform was added to the exosome mixture and it was centrifuged for 5 min at maximum speed (≥10,000 × g) at room temperature. The aqueous (upper) phase was transferred to new tube without lower phase contamination. 1.25 volume of 100% ethanol was added to the aqueous phase. The mixture was placed onto filter cartridge. The filter cartridge with the mixture was centrifuged at 10,000 × g for ~15 s and was washed with wash solution (1, 2 and 3). The filter cartridge was transferred to a fresh collection tube and was eluted with elution solution or nuclease-free water.

Reverse transcription (RT) and pre-amplification

cDNA was generated from exosomal miRNA using Megaplex™ Primer Pools, Human Pools A v2.1 (cat no. 4401009, Thermo Fisher Scientific, Inc.). 3 μL of exosomal miRNA was added to RT reaction mixture (0.80 μL Megaplex™ RT Primers (10×), 0.20 μL dNTPs with dTTP (100 mM), 1.50 μLMultiScribe™ Reverse Transcriptase (50 U/μL), 0.80 μl 10× RT Buffer, 0.90 μL $MgCl_2$ (25 mM), 0.10 μL RNase Inhibitor (20 U/μL) and 0.20 μL Nuclease-free water).

The RT reaction was performed according to the following conditions: 40 cycles of 3 steps (16 ° C for 2 min, 42 ° C for 1 min and 50 ° C for 1 s), hold step for 5 min at 85 ° C and final hold step at 4 ° C. RT reaction was performed in a programmable thermal cycler (PCR system 9700; Thermo Fisher Scientific, Inc.).

To increase the quantity of desired cDNA, preamplification step was performed using Megaplex™ PreAmp Primers, Human Pool A v2.1 (cat no. 4399233, Thermo Fisher Scientific, Inc.). 2.5 μL of RT product was mixed with 22.5 μL of preamplification reaction mixture (TaqMan® PreAmp Master Mix (2×) 12.5 μL, Megaplex™ PreAmp Primers (10×) 2.5 μL, Nuclease-free water 7.5 μL). The preamplification reaction was performed according to the following conditions: Three hold step (95°C for 10 min, 55°C for 2 min and 72°C for 2 min), 12 cycles of 2 steps (95°C for 15 s and 60°C for 4 min), hold step for 10 min at 99.9°C and final hold step at 4°C. RT reaction was performed in a programmable thermal cycler (PCR system 9700; Thermo Fisher Scientific, Inc.).

Quantitative Real-Time polymerase chain reaction (qRT-PCR)

1.33 μL of Preamplified product was added to Universal PCR master mixture using TaqMan™ MicroRNA Assay (cat no.4427975, Thermo Fisher Scientific, Inc.). PCR master mixture was composed with TaqMan MicroRNA Assay (20×) 1.00 μL, TaqMan 2× Universal PCR Master Mix, No AmpErase UNG. 10.00 μL and Nuclease-free water 7.67 μL. TaqMan MicroRNA Assay (20×) were ordered hsa-miR-193a (cat no.002281) and hsa-let-7g (cat no.002282). The PCR amplification was performed according to the following conditions: Initial hold for 10 mins at 95°C, denaturation at 95°C for 15 s, annealing/extension at 60°C for 60 s 25 cycles, followed by a final data collection step at 60°C. PCR amplification was performed in a Applied Biosystems 7300 Fast Real-Time PCR System (Thermo Fisher Scientific, Inc.). *MMP16* and *CDKN1A* genes were performed by traditional qRT-PCR using SYBR green. qRT-PCR mixture (10.0 μL SYBR green 2×, 0.6 μL *MMP16* primer and *CDKN1A* primer and 6.8 μL Distilled water) was added to the complementary DNA (cDNA) 2 μL of cell lines. Sequence of *MMP16* was Forward: TGCCATATGGTGGGAAGATG and Reverse: GTGGACGAAAGCTCCCTGAG. Sequence

of *CDKN1A* was Forward: AGGGGACAGCAGAGGAAG and Reverse: GCGTTTGGAGTGGTAGAAATCTG. The PCR amplification was performed according to the following conditions: Initial hold for 10 min at 95°C, denaturation at 95°C for 15 s, annealing/extension at 57°C for 60 s 40 cycles, followed by a final data collection step at 57°C. PCR amplification was performed in a Applied Biosystems 7300 Fast Real-Time PCR System (Thermo Fisher Scientific, Inc.).

MicroRNA mimic transfection

1×10^6 cells were seeded to be 60-80% confluent on 6-well plate (SPL life sciences). 9 μL Lipofectamine® RNAiMAX Reagent (cat no. 13778100, Thermo Fisher Scientific, Inc.) and 3 μL miRNA mimic of hsa-miR-193a-5p (miRBase accession no. MIMAT0004614, Thermo Fisher Scientific, Inc.) and hsa-let-7g-5p (miRBase accession no. MI0000433, Thermo Fisher Scientific, Inc.) were diluted in 150 μL Opti-MEM Medium, respectively. The diluted miRNA was added to the diluted Lipofectamine® RNAiMAX Reagent (1:1 ratio). The mixture was incubated for 5 min at room temperature. The incubated miRNA-lipid complex was added to

cells. The transfected cell was incubated for 1–3 days in a humidified incubator at 37°C containing 5% CO_2 and 95% air.

Cell invasion assay using 3D cell culture chip

Cell migration assay was performed using the AIM Biotech 3D Cell Culture Chips (cat. no. DAX01; Merck KGaA), according to the manufacturer's instructions (https://www.aimbiotech.com/adherent-cell-migration.html). 1×10^5 cells/mL in Opti-MEM was trypsinized and re-suspended. The cell suspension was mixed with Geltrex® Basement Membrane Matrix gel (cat no. A14132-02, Thermo Fisher Scientific, Inc.). 10 μL of the mixture (with cells) was filled the chip of middle inlet. Gel-filled chips (on AIM holders) was placed into a 37 ℃ incubator and was incubated for half an hour to allow polymerization of collagen to take place. To induce chemotaxis, 50 μL of serum-free cell culture medium was added into one port of a channel and then 50 μL of cell culture medium (with serum) was added to the opposite connected port.

3D Objects Counter plugin (http://fiji.sc/3D_Objects_Counter) in

ImageJ was used to count the total number of cells and to obtain the individual Cartesian coordinates of every cells that has invaded and migrated into the gel. The threshold level and size filter were adjusted to make sure every cell in the region of interest is counted. The differences of the x-coordinates were calculated between cells and the gel interface. Scatter plot was performed by using Graphpadprism (version 5.0). The y-coordinate of the scatter plot represents the invasion distance from the gel interface.

Immunocytochemistry

2×10^5 cells were placed on 8-well Chambered Coverglass with non-removable wells (cat no. 155411, Thermo Fisher Scientific, Inc.) and incubated for 24 h. Cells were permeablilized and fixed with BD Cytofix/Cytoperm™ reagent (cat no. 554722, Thermo Fisher Scientific, Inc.) at room temperature for 20 min. After permeabilization and fixation, cells were treated with 0.1% PBST (phosphate-buffered saline with Tween-20) containing 1% bovine serum albumin for at least 30 min. After the blocking step, cells were incubated with the Alexa Fluor® 568 conjugated anti-Ki67

antibody (RRID:AB_2756822, cat no. ab211968, Abcam) for 2 h at room temperature and with 1 × DAPI solution for 40 min. Immunocytochemistry was performed by LSM800 confocal microscope (Carl Zeiss, Mainz, Germany).

Western blot

Cells were lysed with RIPA lysis buffer (ATTO Corporation) and protein concentrations were determined using the SMART™ Micro BCA Protein Assay kit (Intron Biotechnology, Inc.). Proteins (10 μg) were loaded on Mini-PROTEAN® TGX Precast Gels (Bio-Rad Laboratories, Inc.) with 4× SDS buffer and transferred to PVDF membranes using the Trans-Blot Turbo™ Transfer Pack (Bio-Rad Laboratories, Inc.). The membranes were blocked at room temperature for 1 h with 2% skim milk in 0.05% TBS-Tween (BD Biosciences) and were then exposed to primary antibodies for 1–2 h at room temperature against CD63 (RRID: AB_2800495 , cat. no. 134045; 1:1000; Abcam, UK), Calnexin (RRID:AB_2864299 , cat. no. ab133615, 1:2000; Abcam, UK) MMP16 (RRID:AB_2532467, cat. no. 701306; 1:2000; Thermo Fisher Scientific, Inc.), E-

cadherin (RRID:AB_300946, cat no. ab1416; 1:500; Abcam, UK), total ERK (RRID:AB_330744, cat. no. 9102; 1:1,000; Cell Signaling Technology, Inc.), phosphorylated (p)-ERK (RRID:AB_331646, cat. no. 9101; 1:250; Cell Signaling Technology, Inc.), Snail (RRID:AB_2255011, cat no. 3879; 1:1000; Cell Signaling Technology, Inc.), Vimentin (RRID:AB_10562134, cat no. ab92547; 1:2000; Abcam) and β-actin (RRID:AB_2714189, cat. no. sc-47778; 1:100; Santa Cruz Biotechnology, Inc.). Subsequently, membranes were incubated with anti-mouse IgG (H+L) secondary antibody, HRP (RRID:AB_2536527, cat. no. G-21040; 1:5,000; Thermo Fisher Scientific, Inc.) and anti-rabbit IgG (H+L) secondary antibody, HRP (RRID:AB_1500696, cat. no. G-21234; 1:5,000; Thermo Fisher Scientific, Inc.). ECL reagent (Pierce™ ECL Western Blotting Substrate; cat no. 32106; Thermo Fisher Scientific, Inc.) was used for visualization. β-actin was used as a loading control for each lane. All results were quantified using ImageJ 1.8.0 (https://imagej.nih.gov/ij/).

Drug sensitivity test

AUC value of CRC-PTM cell lines. The experiment was conducted as described in the previous paper (32). At density of 2×10^5 cells/well, tumor cells were seeded into a 96-well plate. Optimal concentrations of anti-cancer drugs were then used to treat 18 CRCs. These concentrations were: 100 μg/mL of TAS-102, 100 μg/mL of Regorafenib, 1000 μg/mL of Leucovorin calcium, 1000 μg/mL of Capecitabine, 50 μg/mL of Apitolisib, 100 μg/mL of Belinostat, 50 μg/mL of Trametinib, 50 μg/mL of Cyclopamine, 100 μg/mL of ICG-001, 100 μg/mL of Buparlisib, 50 μg/mL of SAHA, 50 μg/mL of Afatinib, 5 μg/mL of AZD2014, 100 μg/mL of MK-5108, 50 μg/mL of Olaparib, 100 μg/mL of Irinotecan, 50000 μg/mL of 5-FU, 100 μg/mL of Oxaliplatin, 100 μg/mL of Baicalein, 100 μg/mL of Curcumin, 100 μg/mL of Genistein, 200 μg/mL of Resveratrol, 1000 μg/mL of Cetuximab, and 1000 μg/mL of Bevacizumab. The 96-well plate containing anti-cancer drugs was incubated for 72 h at 37 ℃. After incubation, 10 uL EZ-Cytox solution was applied to each well. After the plate was incubated for 2 h at 37 ℃, optical density value was assessed at 450 nm with a Multiskan™ GO Microplate Spectrophotometer

(Thermo Fisher Scientific).

Live/Dead cell counts of miRNA mimic treatment. 2×10^5 cells were placed on 96-well plate (cat no. 30096, SPL life sciences, USA). After incubation for 24 h, cells were stained with 4 μg/mL of Hoechst 33342 (cat no. H3570, Thermo Fisher Scientific, Inc.) for 30–60 min. Hoechst 33342 was aspirated and mixture of anti-cancer drugs and 4 μg/mL propidium iodide was treated to the cell. Anti-cancer drugs treated on cells were selected as Afatinib, AZD2014, 5-Fu, Oxaliplatin, Regorafenib, Trametinib, Cylcopamine and ICG-001. These concentrations were: 50 μg/mL of Afatinib, 5 μg/mL of AZD2014, 50000 μg/mL of 5-FU, 100 μg/mL of Oxaliplatin, 100 μg/mL of Regorafenib, 50 μg/mL of Trametinib, 50 μg/mL of Cyclopamine, 100 μg/mL of ICG-001. After treatment with the mixture, the bright field, Hoechst 33342 and propidium iodides of cells were observed every 24, 48, and 72 h through the ImageXpress Micro Confocal High-Content Imaging System (Molecular Devices, LLC., USA). The number and percentage of Live/Dead cells were calculated with the MetaXpress software

version 6 (provided with the ImageXpress instrument).

Microarray of microRNA and mRNA expression

The Affymetrix Genechip miRNA 4.0 array process was executed according to the manufacturer's protocol. 1000 ng RNA samples were labeled with the FlashTag™ Biotin RNA Labeling Kit (Genisphere, Hatfield, PA, USA). The labeled RNA was quantified, fractionated and hybridized to the miRNA microarray according to the standard procedures provided by the manufacture. The labeled RNA was heated to 99℃ for 5 minutes and then to 45 ℃ for 5 min.

RNA-array hybridization was performed with agitation at 60 rotations per minute for 16 h at 48 ℃ on an Affymetrix GeneChip Hybridization oven 645. The chips were washed and stained using a Genechip Fluidics Station 450 (Affymetrix, CA, USA). The chips were then scanned with an Affymetrix GCS 3000 canner (Affymetrix).

MiRNA-Gene ontology (GO) analysis was performed by top 5 list of miRNAs that satisfy $|\text{fold change}| \geq 2$ and p value < 0.05 between primary CRC group and paired PTM group. The miRNA-GO

analysis was conducted through DIANA-mirPath v 3.0 software.

The genes targeted by miR-193a used heatmap to compare the expression levels in each CRC-PTM cell line set (SNU-2335A, SNU-2335D, SNU-2404A, SNU-2404B, SNU-2414A and SNU-2414B) and the heatmap were analyzed using "pheatmap" libarary in R program (v 4.0.0).

Microarray raw data preparation and Statistical analysis

Raw data were extracted automatically in Affymetrix data extraction protocol using the software provided by Affymetrix GeneChip® Command Console® Software (AGCC). The CEL files import, miRNA level RMA+DABG-All analysis and result export using Affymetrix® Power Tools (APT) Software. Array data were filtered by probes annotated species.

The comparative analysis between test sample and control sample was carried out using independent t-test and fold change in which the null hypothesis was that no difference exists among groups. False discovery rate (FDR) was controlled by adjusting p value < 0.05 using Benjamini-Hochberg algorithm. All Statistical test and

visualization of differentially expressed genes was conducted using R statistical language 3.3.2 (https://www.r-project.org/).

RESULTS

Isolation and validation of exosomal miRNA in CRC and PTM cell lines

Three pairs of primary CRC and PTM cell lines (SNU-2335A, SNU-2335D, SNU-2404A, SNU-2404B, SNU-2414A and SNU-2414B) originating from the same patient were all grown in attached form, except for the floating cells, SNU-2404B. All six cell lines were shown to have the shape of typical epithelial cells (Figure 1A).

To identify the exosome extraction without cell lysates contamination, the exosomes extracted from the primary colorectal cancer and peritoneal metastatic cell lines were confirmed using CD63 (exosome positive marker), and Calnexin (exosome negative marker) (33), respectively (Figure 1B). Cell lysate was used as an internal positive control, CD63 was confirmed to be positive in all cell lines, and there was no contamination of cell lysate by negative of Calnexin.

The similarity of exosomal miRNAs between the CRC and the

paired PTM was confirmed by multidimensional scaling (MDS). The exosomal miRNA dataset showed a low level of similarity in the SNU-2404 set and the SNU-2414 set, except for the SNU-2335 set (Figure 1C). Common exosomal miRNAs with significant fold changes between CRC and PTM groups were let-7g-5p, miR-191-5p, miR-193a-5p, miR-4674, and miR-6789-5p. Let-7g-5p and miR-191-5p increased in the PTM group as compared to the CRC group, and miR-193a-5p, miR-4674 and miR-6789-5p decreased in the PTM group as much as in the CRC group (Figure 1D).

The top 5 exosomal miRNAs were sorted with a significant fold change in the SNU-2335 set, SNU-2404 set and the SNU-2414 set (table1). A total of 16 miRNAs were sorted, including the pan-CRC-PTM group (except that the 4 exosomal miRNAs that had been duplicated).

A total of 16 exosomal miRNAs were analyzed to perform physiological functions in the cell through DIANA-miRPath GO analysis. This confirmed that 16 exosomal miRNAs were involved

in various biological processes, including gene expression, cell-cell signaling, extracellular matrix organization, and disassembly (Figure 1E).

To validate both the let-7g-5p and miR-193a-5p among the exosomal miRNAs having significant fold changes, it was confirmed that miR-193a showed a significant difference among all CRC-PTM sets (including the primary CRC-lymph node metastasis set) through qRT-PCR. On the other hand, let-7g-5p was found to have no significant difference between the SW480-620 set and the KM12C-KM1214 set (Figure 1F-G).

Figure 1

(A)

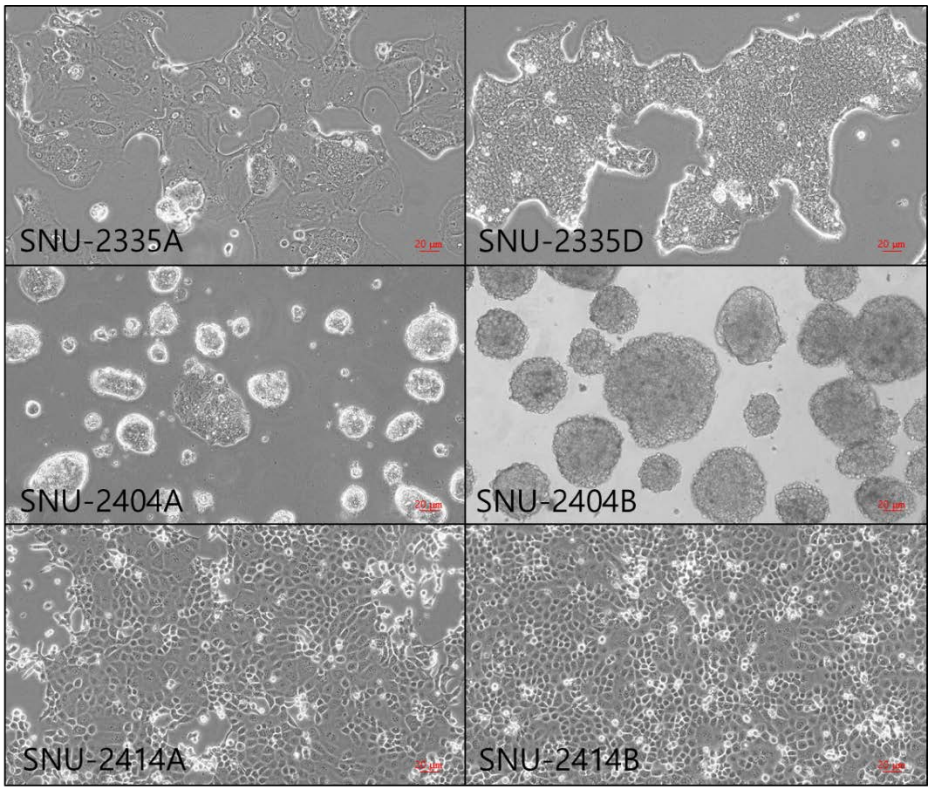
SNU-2335A
SNU-2335D
SNU-2404A
SNU-2404B
SNU-2414A
SNU-2414B

(B)

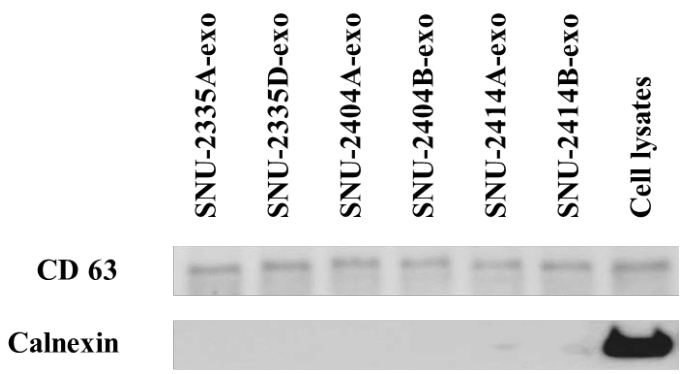
SNU-2335A-exo
SNU-2335D-exo
SNU-2404A-exo
SNU-2404B-exo
SNU-2414A-exo
SNU-2414B-exo
Cell lysates
CD 63
Calnexin

(C)

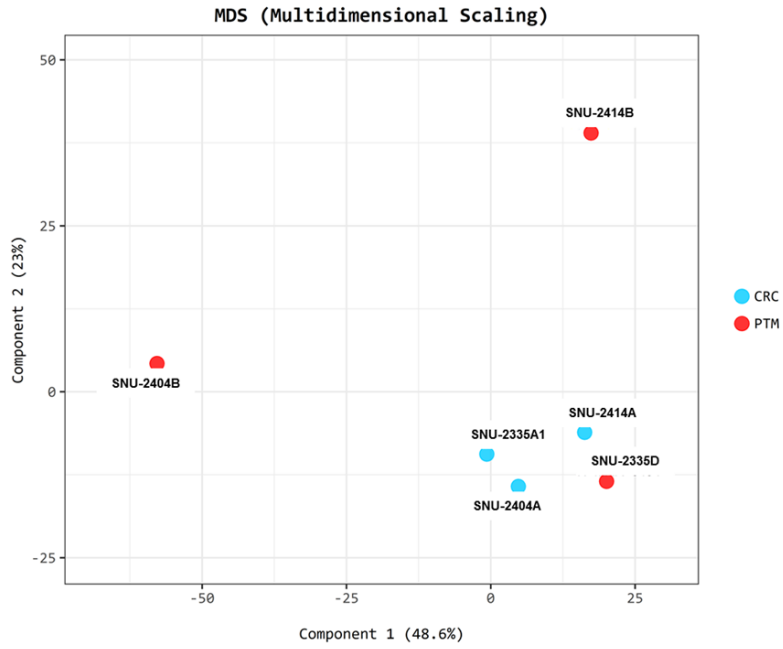
MDS (Multidimensional Scaling)
Component 2 (23%)
Component 1 (48.6%)
SNU-2414B
SNU-2404B
SNU-2414A
SNU-2335A1
SNU-2335D
SNU-2404A
CRC
PTM

(D)

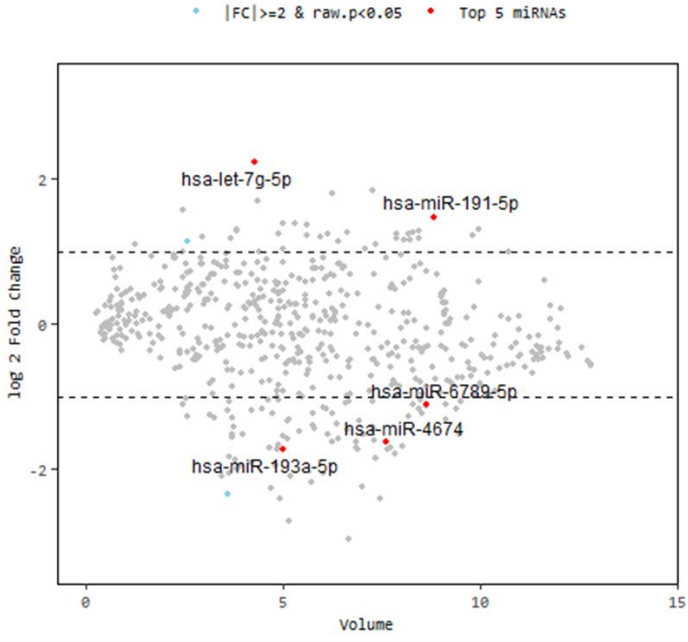
|FC|>=2 & raw.p<0.05
Top 5 miRNAs
log 2 Fold Change
Volume
hsa-let-7g-5p
hsa-miR-191-5p
hsa-miR-6789-5p
hsa-miR-4674
hsa-miR-193a-5p

(E)

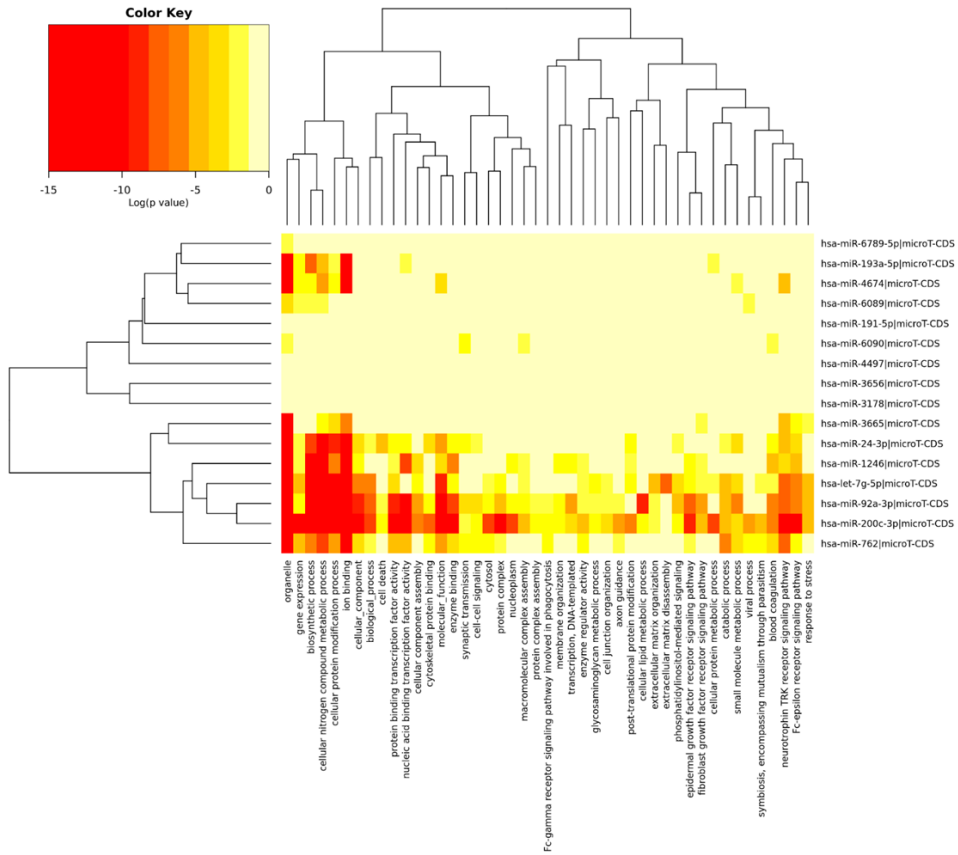
Color Key
-15
-10
-5
0
Log(p value)
hsa-miR-6789-5p|microT-CDS
hsa-miR-193a-5p|microT-CDS
hsa-miR-4674|microT-CDS
hsa-miR-6089|microT-CDS
hsa-miR-191-5p|microT-CDS
hsa-miR-6090|microT-CDS
hsa-miR-4497|microT-CDS
hsa-miR-3656|microT-CDS
hsa-miR-3178|microT-CDS
hsa-miR-3665|microT-CDS
hsa-miR-24-3p|microT-CDS
hsa-miR-1246|microT-CDS
hsa-let-7g-5p|microT-CDS
hsa-miR-92a-3p|microT-CDS
hsa-miR-200c-3p|microT-CDS
hsa-miR-762|microT-CDS
organelle
gene expression
biosynthetic process
cellular nitrogen compound metabolic process
cellular protein modification process
ion binding
cellular_component
biological_process
cell death
protein binding transcription factor activity
nucleic acid binding transcription factor activity
cellular component assembly
cytoskeletal protein binding
molecular_function
enzyme binding
synaptic transmission
cell-cell signaling
cytosol
protein complex
nucleoplasm
macromolecular complex assembly
protein complex assembly
Fc-gamma receptor signaling pathway involved in phagocytosis
membrane organization
transcription, DNA-templated
enzyme regulator activity
glycosaminoglycan metabolic process
cell junction organization
axon guidance
post-translational protein modification
cellular lipid metabolic process
extracellular matrix organization
extracellular matrix disassembly
phosphatidylinositol-mediated signaling
epidermal growth factor receptor signaling pathway
fibroblast growth factor receptor signaling pathway
cellular protein metabolic process
catabolic process
small molecule metabolic process
viral process
symbiosis, encompassing mutualism through parasitism
host cell cytoplasm
neurotrophin TRK receptor signaling pathway
Fc-epsilon receptor signaling pathway
response to stress

(F)

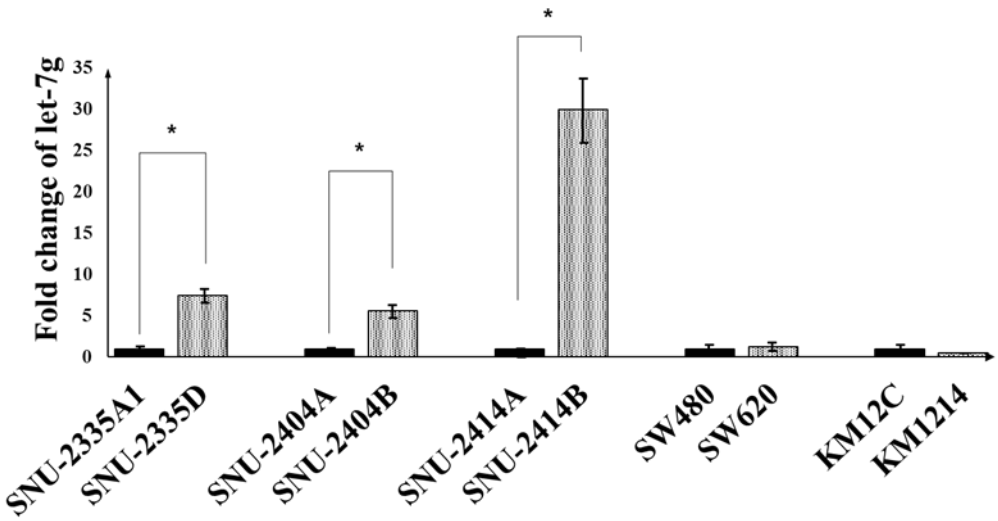
Fold change of let-7g
35
30
25
20
15
10
5
0
*
*
*
SNU-2335A1
SNU-2335D
SNU-2404A
SNU-2404B
SNU-2414A
SNU-2414B
SW480
SW620
KM12C
KM1214

(G)

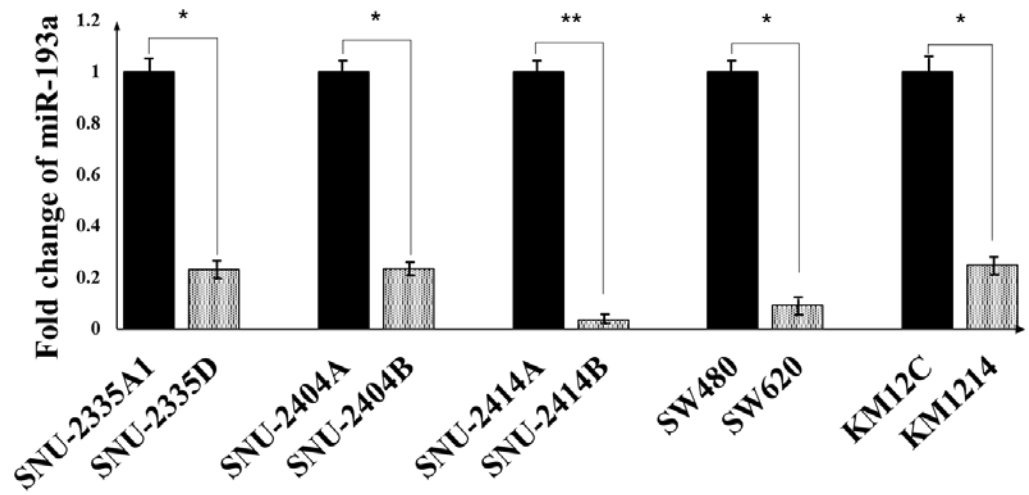
Fold change of miR-193a
1.2
1
0.8
0.6
0.4
0.2
0
*
*
**
*
*
SNU-2335A1
SNU-2335D
SNU-2404A
SNU-2404B
SNU-2414A
SNU-2414B
SW480
SW620
KM12C
KM1214

Figure 1. Isolation and validation of exosomal miRNA between primary CRC and paired PTM

The morphological characteristics of primary colorectal cancer cell lines and peritoneal metastatic colorectal cell lines were observed under a microscope. Primary colorectal cancer: (A) SNU-2335A, SNU-2404A, SNU-2414A; Peritoneal metastatic cancer: SNU-2335D, SNU-2404B, SNU-2414B. (B) CD63 was used as a positive marker for exosome, and Calnexin (endoplasmic reticulum marker) was used as a negative marker. To confirm the contamination of cell lysate, cell lysate was used as an internal control. (C) MDS plot was visualized the level of similarity of individual cases of a dataset. Blue dot: primary CRC group, Red dot: PTM group. (D) Top 5 list of miRNAs that satisfy |fold change| $\geq$ 2 and $p < 0.05$ between primary CRC group and paired PTM group. (E) Gene ontology analysis was performed through DIANA-mirpath v3.0 software to identified what role the total of 16 miRNAs present in the top5 list (except 4 duplicated miRNAs) played in the cell. A total of 16 miRNAs were involved in functions such as ECM

disassembly and organization. (F–G) Let–7g–5p and miR–193a–5p were selected as miRNAs with higher and lower fold change in the peritoneal metastasis group than the primary colorectal cancer group out of a total of 16 miRNAs. qRT–PCR was performed to confirm that miR–193a showed a significant difference in all cell line sets. Data is presented by t–test as compared to primary CRC cell line. $*p < 0.05$ and $**p < 0.01$. $n = 3$. (F) fold change of let–7g, (G) fold change of miR–193a.

Table 1. Exosomal miRNA Top 5 list of microarray data

SNU-2335 set	**SNU-2404 set**	**SNU-2414 set**	**CRC vs PTM**
hsa-miR-24-3p	hsa-miR-762	hsa-miR-3178	hsa-let-7g-5p
hsa-miR-92a-3p	hsa-miR-1246	hsa-miR-3665	hsa-miR-191-5p
hsa-miR-200c-3p	hsa-miR-3656	hsa-miR-4497	hsa-miR-193a-5p
hsa-miR-1246	hsa-miR-6089	hsa-miR-6089	hsa-miR-4674
hsa-miR-3178	hsa-miR-6090	hsa-miR-6090	hsa-miR-6789-5p

MMP16 and *CDKN1A* as exosomal miRNA target genes

The target genes of miR-193a-5p were predicted through MicroRNA Target Prediction Database (miRDB), TargetScan v7.2 and miRWalk 2.0. Both *MMP16* and *CDKN1A* were sorted as a result of using three prediction analysis methods (table2). To elucidate the effect of miRNA mimic on cell signaling pathway, the metastatic cell line treated with miR-193a mimicked the decreased RNA expression of *MMP16* as compared to the metastatic cell line of the control group in all CRC-PTM cell line sets with the SW480-620 set and the KM12C-1214 set (lymph node metastasis) (Figure 2A). The primary CRC cell lines with let-7g mimicked a more significantly decreased *CDKN1A* expression than did the cell lines of the control group in all cell lines except KC12C (Figure 2B).

The protein expression of MMP16 was also lower in the primary CRC group than in the metastasis group in the CRC-PTM cell line set. In comparison, SW480-620 set and KC12C-1214 set showed no significant differences in protein expression. The peritoneal metastatic cell line treated with miR-193a mimicked increased

protein expression of E-cadherin more than did the control peritoneal metastasis cell line in SNU-2335D and SNU-2404B. Snail and vimentin were shown to be opposite to the expression of E-cadherin, and snail and vimentin expressions of the peritoneal metastatic cell line treated with miR-193a mimic were more decreased than were the control peritoneal metastatic cell line in SNU-2335D, SNU-2404B and SNU-2414B. Phospho-ERK expression of the peritoneal metastatic cell line group did not show any significant difference in the effects of the miR-193a mimic (Figure 2C). The phospho-ERK expression of the let-7g treatment group was higher than that of the control group in SNU-2404A and SNU-2414A. There was no significant difference in the expression of EMT markers, including E-cadherin or snail and vimentin, between the primary CRC cell line group and the let-7g treatment group (Figure 2D).

Table 2. Exosomal let−7g and miR−193a targeted gene list

miRNA ID	refseqid	genesymbol	start	end	binding_region_length	longest_consecutive_pairings	position
hsa-miR-193a-5p	NM_001111067	*ACVR1*	17	66	20	7	5UTR
hsa-miR-193a-5p	NM_001111067	*ACVR1*	1815	1840	25	8	3UTR
hsa-miR-193a-5p	NM_001105	*ACVR1*	1996	2021	25	8	3UTR
hsa-miR-193a-5p	NM_001105	*ACVR1*	545	570	25	7	CDS
hsa-miR-193a-5p	NM_001105	*ACVR1*	1371	1411	40	8	CDS
hsa-miR-193a-5p	NM_001105	*ACVR1*	1871	1890	19	13	CDS
hsa-miR-193a-5p	NM_001347667	*ACVR1*	1905	1930	25	8	3UTR
hsa-miR-193a-5p	NM_001347667	*ACVR1*	454	479	25	7	CDS
hsa-miR-193a-5p	NM_001347667	*ACVR1*	1280	1320	40	8	CDS
hsa-miR-193a-5p	NM_005941	*MMP16*	448	487	20	11	CDS
hsa-let-7g-5p	XM_024447658	*TGFBR1*	915	936	21	16	5UTR
hsa-let-7g-5p	NM_001220777	*CDKN1A*	286	305	19	13	CDS
hsa-let-7g-5p	NM_078467	*CDKN1A*	288	307	19	13	CDS
hsa-let-7g-5p	NM_000389	*CDKN1A*	341	360	19	13	CDS
hsa-let-7g-5p	NM_001220778	*CDKN1A*	451	470	19	13	CDS

The results of the analysis were integrated using three target prediction programs: miRDB, miRwalk, and Targetscan.

Figure 2

(A)

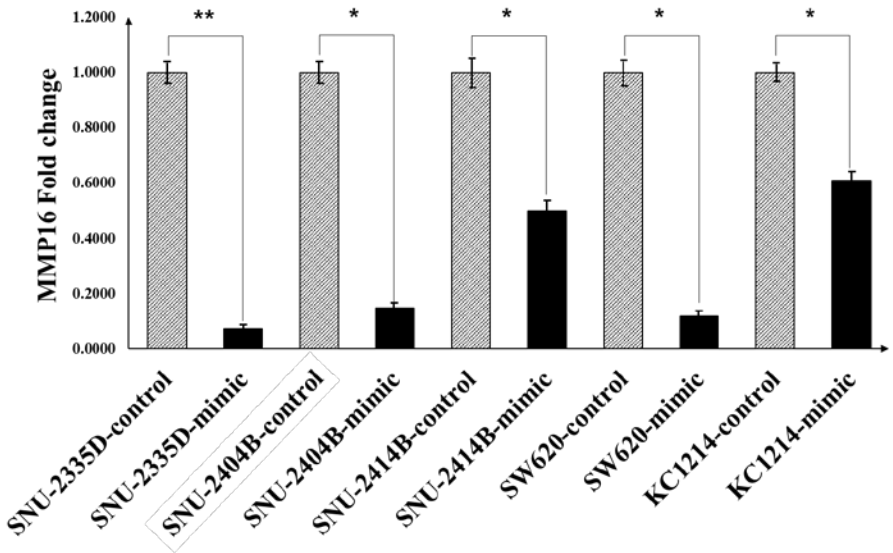
MMP16 Fold change
1.2000
1.0000
0.8000
0.6000
0.4000
0.2000
0.0000
**
*
*
*
*
SNU-2335D-control
SNU-2335D-mimic
SNU-2404B-control
SNU-2404B-mimic
SNU-2414B-control
SNU-2414B-mimic
SW620-control
SW620-mimic
KC1214-control
KC1214-mimic

(B)

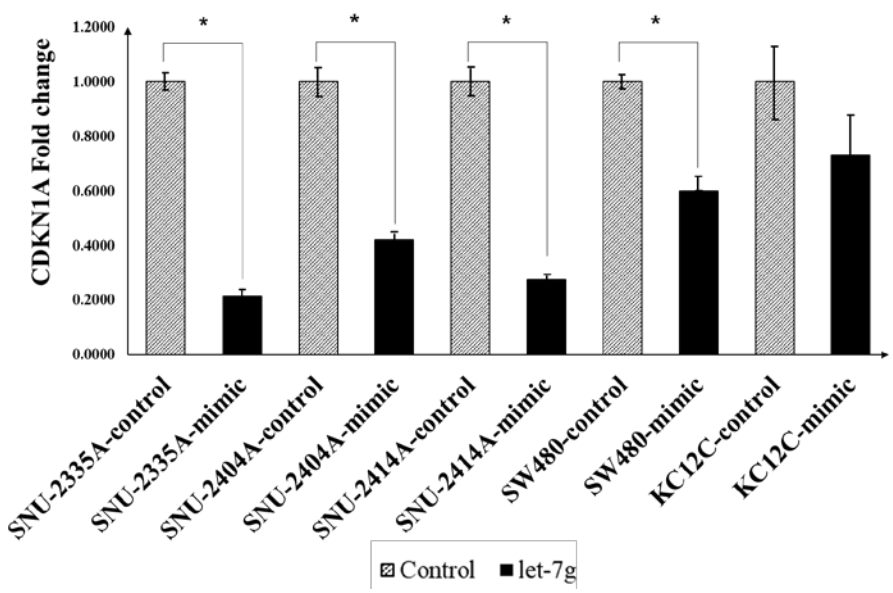
CDKN1A Fold change
1.2000
1.0000
0.8000
0.6000
0.4000
0.2000
0.0000
*
*
*
*
SNU-2335A-control
SNU-2335A-mimic
SNU-2404A-control
SNU-2404A-mimic
SNU-2414A-control
SNU-2414A-mimic
SW480-control
SW480-mimic
KC12C-control
KC12C-mimic
Control
let-7g

(C)

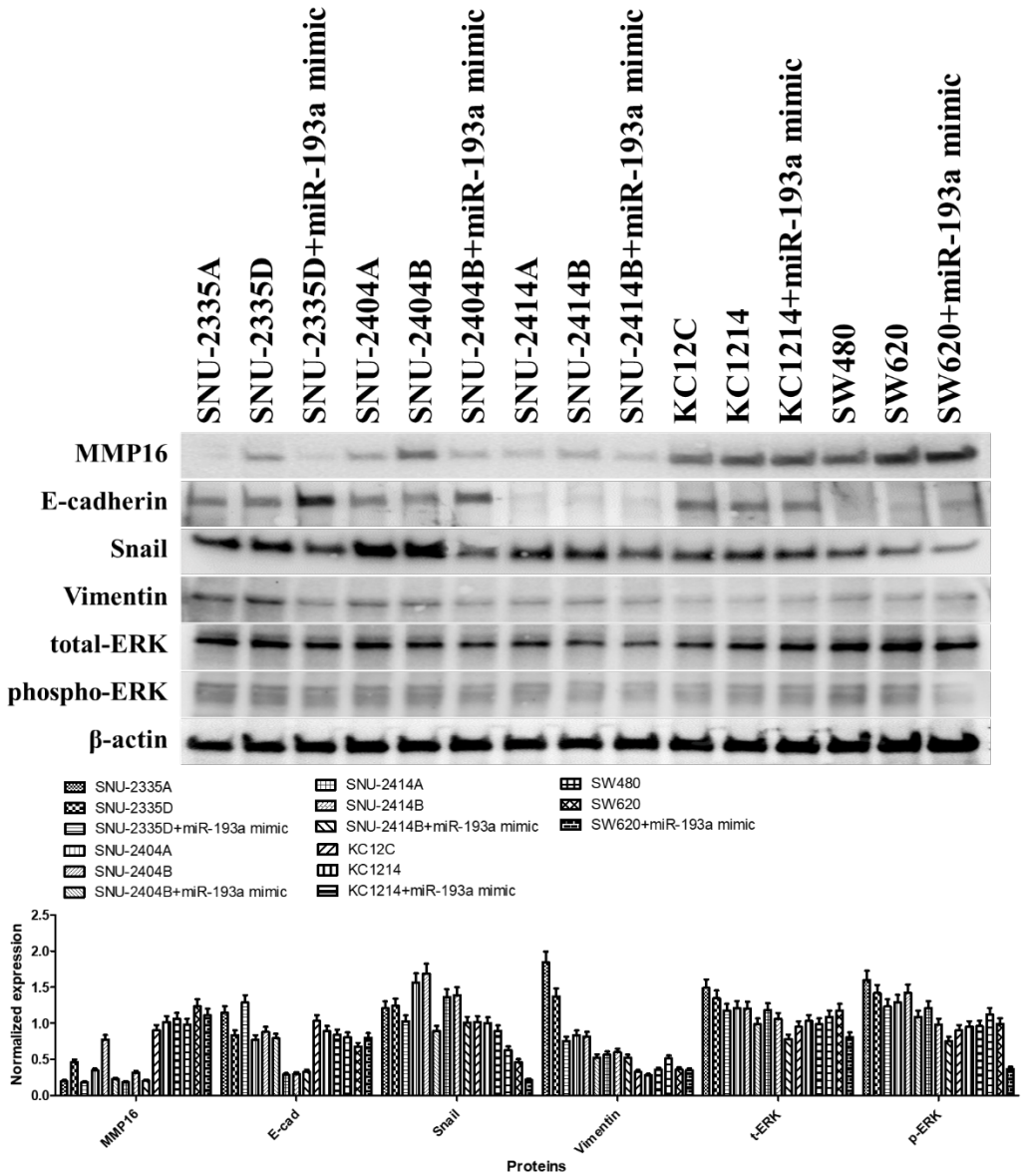
SNU-2335A
SNU-2335D
SNU-2335D+miR-193a mimic
SNU-2404A
SNU-2404B
SNU-2404B+miR-193a mimic
SNU-2414A
SNU-2414B
SNU-2414B+miR-193a mimic
KC12C
KC1214
KC1214+miR-193a mimic
SW480
SW620
SW620+miR-193a mimic
MMP16
E-cadherin
Snail
Vimentin
total-ERK
phospho-ERK
β-actin
Normalized expression
2.5
2.0
1.5
1.0
0.5
0.0
MMP16
E-cad
Snail
Vimentin
t-ERK
p-ERK
Proteins

(D)

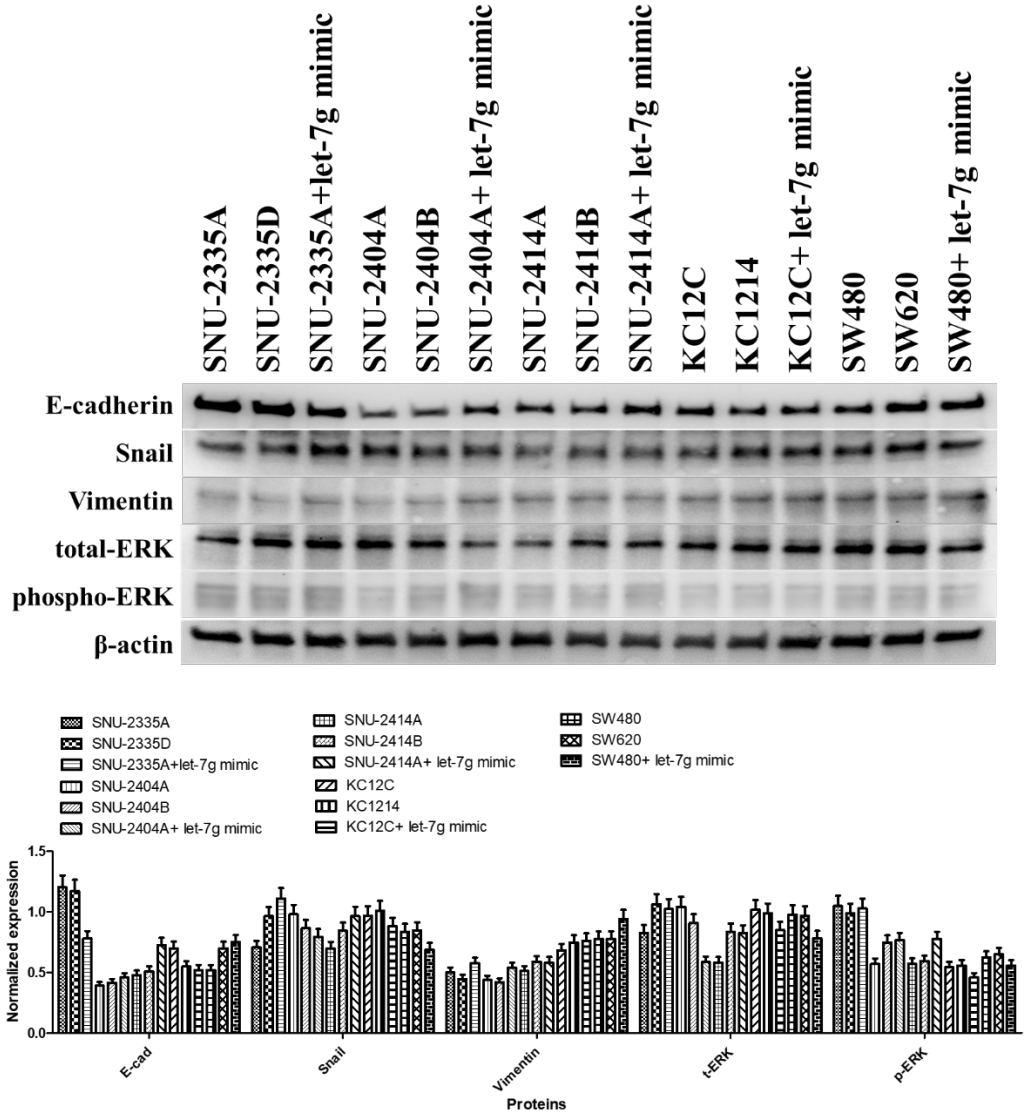
SNU-2335A
SNU-2335D
SNU-2335A+let-7g mimic
SNU-2404A
SNU-2404B
SNU-2404A+ let-7g mimic
SNU-2414A
SNU-2414B
SNU-2414A+ let-7g mimic
KC12C
KC1214
KC12C+ let-7g mimic
SW480
SW620
SW480+ let-7g mimic
E-cadherin
Snail
Vimentin
total-ERK
phospho-ERK
β-actin
Normalized expression
1.5
1.0
0.5
0.0
E-cad
Snail
Vimentin
t-ERK
p-ERK
Proteins

Figure 2. Effect of miR-193a and let-7g on target gene expression in CRC-paired PTM sets

qRT-PCR was performed to compare the difference of *MMP16* in treatment of miR-193a-mimic. SNU-2335 set, SNU-2404 set and SNU-2414 set are peritoneal metastasis case, and KC12C-1214 set and SW480-620 set are lymph node metastasis case. Data is presented by t-test as compared to control group. $*p < 0.05$ and $**p < 0.01$. $n = 3$. (A) *MMP16* mRNA expression of metastatic cell line groups transfected with miR-193a mimic. (B) *CDKN1A* mRNA expression of primary CRC cell line groups transfected with let-7g mimic. (C) Protein expression of metastatic cell line groups transfected with miR-193a mimic. $n = 3$. (D) Protein expression of primary CRC cell line groups transfected with let-7g mimic. β-actin was used as a loading control for each lane. $n = 3$.

Metastatic role of exosomal miR-193a and exosomal let-7g

To elucidate the metastatic role of exosomal miR-193a and let-7g, cell invasiveness was confirmed by inducing chemotaxis. Cell invasion of the right channel was not seen because of chemotaxis from right to left, whereas cell invasion to the left channel was observed in SNU-2335A, SNU-2335D, SNU-2404A, SNU-2404B, SNU-2414A and SNU-2414B. The peritoneal metastatic cell lines expressed miR-193a to a lesser degree and the let-7g to a greater degree than did the primary CRC cell lines. Therefore, in order to confirm the effect of miR-193a, an miR-193a mimic was treated in the metastatic group and compared to the control group. Similarly, to confirm the effect of let-7g, the primary CRC group with an let-7g mimic was compared to the control group. The group treated with the miR-193a mimic significantly decreased cell invasiveness as compared to the control group, and the group treated with the let-7g mimic significantly increased cell invasiveness as compared to the control group (Figure 3A-C).

The inhibitory effect of cell invasiveness by miR-193a was 59.6%,

88.2%, and 54.8%, in the SNU-2335D, SNU-2404B and SNU-2414B, respectively. Conversely, the effect of increasing cell invasiveness by let-7g was 471.7%, 240.1%, and 278.7% in SNU-2335A, SNU-2404A, and SNU-2414A, respectively.

In order to confirm the cell proliferation, the change in intracellular expression of Ki-67 (a cell proliferation marker) was observed in the treatment of miR-193a and the let-7g mimic. Based on the exosomal miRNA analysis between the primary CRC and the PTM groups, the miR-193a expression was lower and let-7g expression was higher after metastasis. Therefore, the let-7g mimic and the miR-193a mimic treatments were performed for the primary CRC group and the PTM group, respectively. Ki-67 expression of the let-7g mimic treatment group increased as compared to the control group in SNU-2335A. The Ki-67 expression of the miR-193a mimic treatment group decreased than that of the control group in SNU-2335D (Figure 3D-E).

Figure 3

(A)

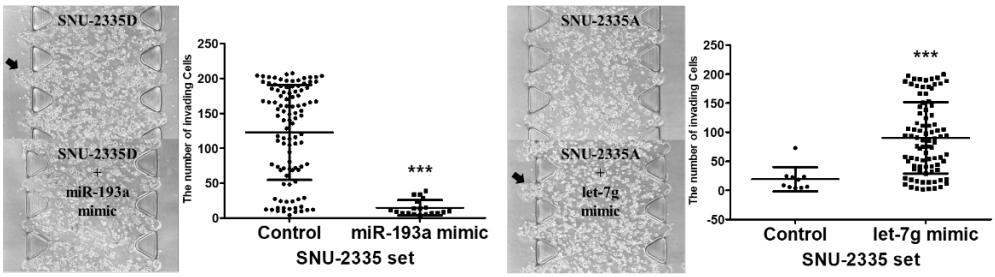
SNU-2335D
SNU-2335D + miR-193a mimic
The number of invading Cells
250
200
150
100
50
0
***
Control
miR-193a mimic
SNU-2335 set
SNU-2335A
SNU-2335A + let-7g mimic
The number of invading Cells
250
200
150
100
50
0
-50
***
Control
let-7g mimic
SNU-2335 set

(B)

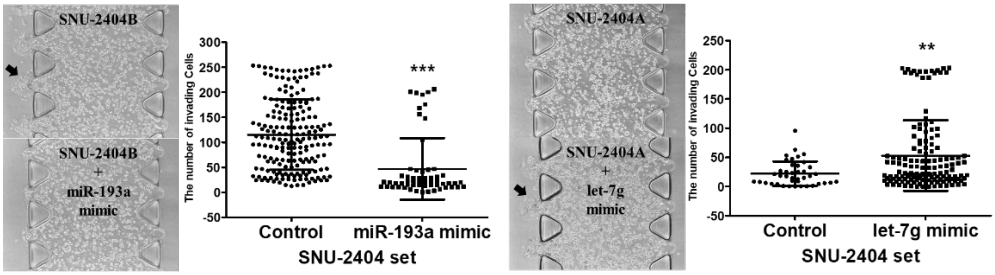
SNU-2404B
SNU-2404B + miR-193a mimic
The number of invading Cells
300
250
200
150
100
50
0
-50
***
Control
miR-193a mimic
SNU-2404 set
SNU-2404A
SNU-2404A + let-7g mimic
The number of invading Cells
250
200
150
100
50
0
-50
**
Control
let-7g mimic
SNU-2404 set

(C)

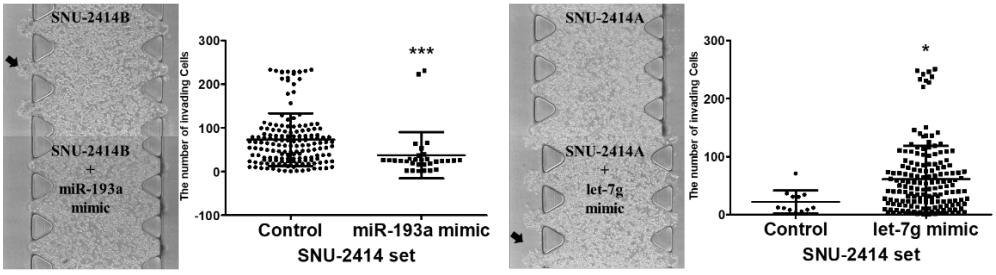
SNU-2414B
SNU-2414B + miR-193a mimic
The number of invading Cells
300
200
100
0
-100
***
Control
miR-193a mimic
SNU-2414 set
SNU-2414A
SNU-2414A + let-7g mimic
The number of invading Cells
300
200
100
0
*
Control
let-7g mimic
SNU-2414 set

(D)

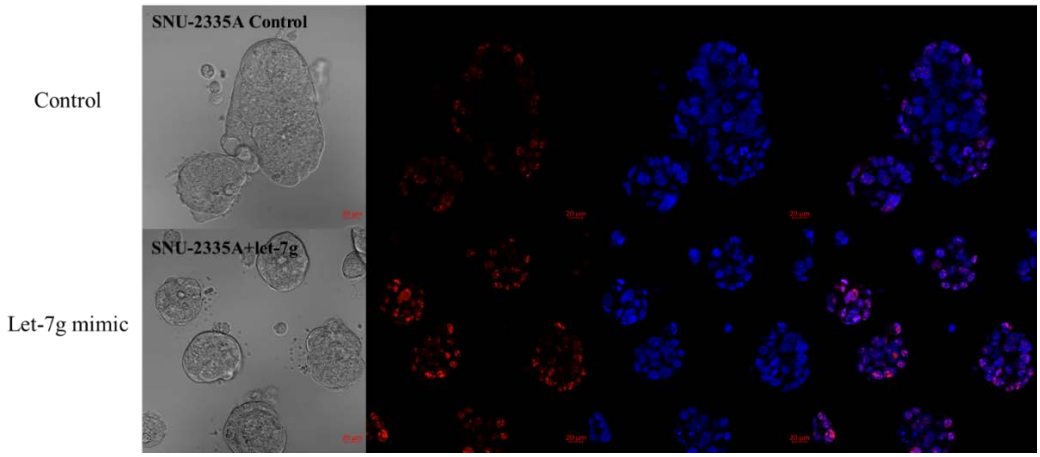
Control
Let-7g mimic
SNU-2335A Control
SNU-2335A+let-7g

(E)

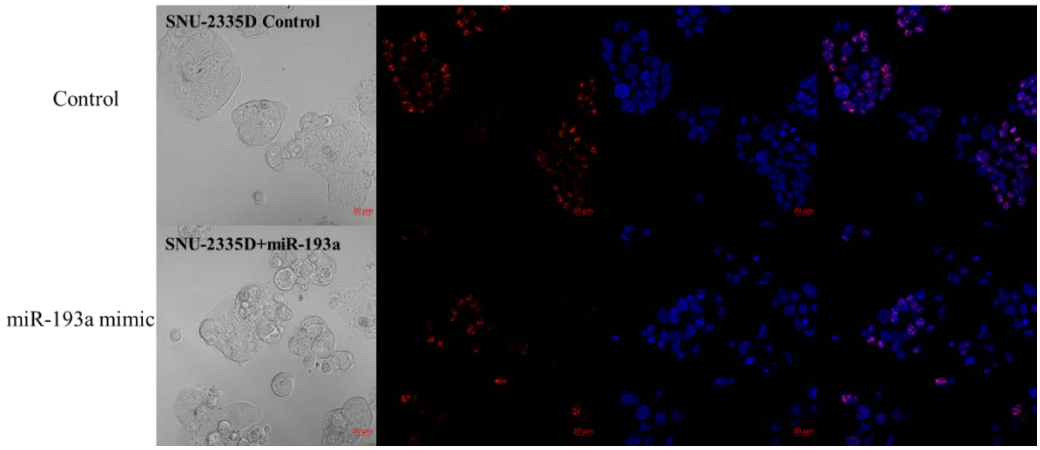
Control
miR-193a mimic
SNU-2335D Control
SNU-2335D+miR-193a

Figure 3. Effect of miR-193a and let-7g mimic on metastatic properties

Cell invasiveness was measured by inducing chemotaxis from right to left by cells mixed with BME gel in the middle channel. The y-coordinate of the scatter plot represents the invasion distance from the gel interface. Data is presented by t-test as compared to control group. $*p < 0.05$, $**p < 0.01$ and $***p < 0.001$. $n = 3$. (A) left: SNU-2335D+miR-193a mimic, right: SNU-2335A+let-7g mimic; (B) left: SNU-2404B+miR-193a mimic, right: SNU-2404A+let-7g mimic; (C) left: SNU-2414B+miR-193a mimic, right: SNU-2414A+let-7g mimic.

Ki-67 expression was performed by confocal microscope. Left to right image: Bright field, Red: Ki-67, Blue: DAPI and merged image. (D) SNU-2335A, (E) SNU-2335D.

Analysis of multiple drug responsiveness for clinical approach

In most drugs, metastatic cell lines survived at higher drug concentrations as compared to primary colorectal cancer cell lines (Figure 4A). A total of six cell lines was generally sensitive to receptor tyrosine kinase inhibitors, such as regorafenib and afatinib, and also were sensitively affected by MEK inhibitors such as trametinib. On the other hand, cell lines showed relatively high AUC values for AZD2014 known as an mTOR inhibitor, oxaliplatin known as one element of the FOLFOX (typically along with folinic acid and 5-fluorouracil). Among 24 drugs, five drugs with a low AUC value (regorafenib 1.92 ± 0.71, 5-Fu 1.69 ± 0.59 and trametinib 1.87 ± 0.33), one drug with a middle AUC value (ICG-001 2.1 ± 0.24, afatinib 2.13 ± 0.47 and cyclopamine 2.49 ± 0.25) and two drugs with a high AUC value (AZD2014 2.66 ± 0.37 and oxaliplatin 2.5 ± 0.18) were selected to analyze the drug response to the cell lines treated with an miRNA mimic (Figure 4B-C). After treatment with the drugs, the PI was continuously increased for three days, and the number of dead cells was confirmed by increasing the PI in all cell

lines (Figure 4B). Comparing the percentage of living cells according to the AUC type of drug, the miRNA mimic-treated cell lines for two drugs, oxaliplatin and regorafenib, which respectively had a high and low AUC value on average, also showed the same pattern. Of note, the AUC value of AZD2014 was higher than that of 5-Fu and trametinib. But cell viability with AZD2014 treatment was lower than the treatment with 5-Fu and trametinib in drug response tests, including the miRNA mimic treated group (Figure 4C).

Figure 4

(A)

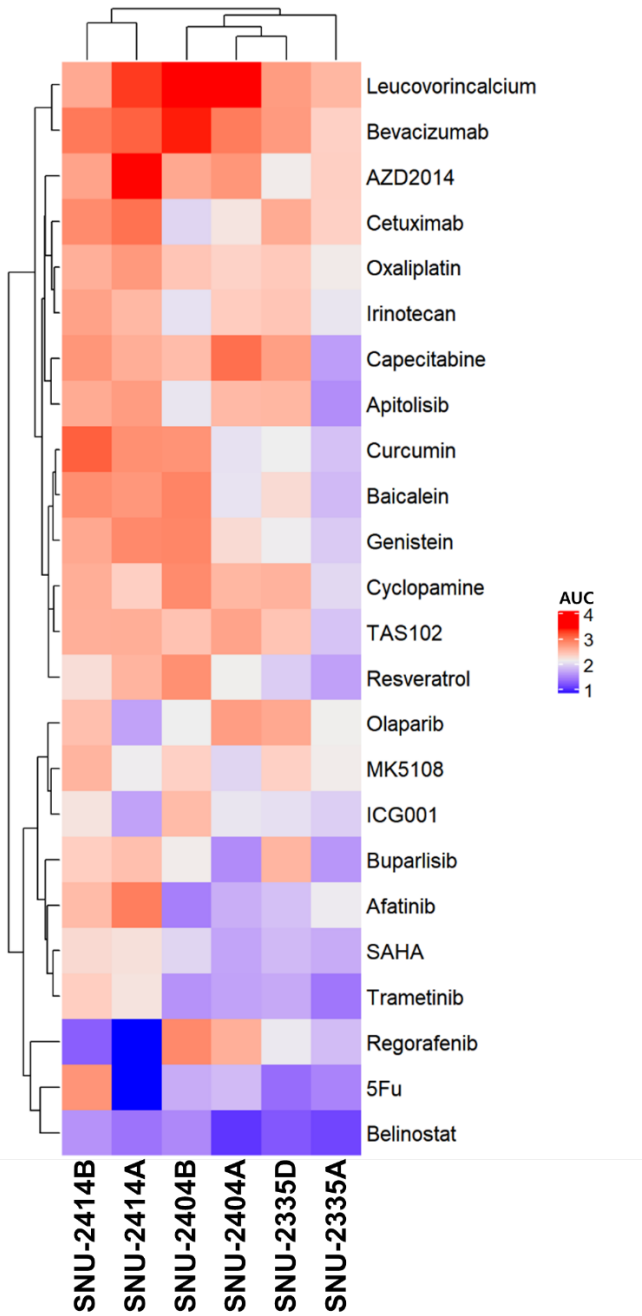
Leucovorincalcium
Bevacizumab
AZD2014
Cetuximab
Oxaliplatin
Irinotecan
Capecitabine
Apitolisib
Curcumin
Baicalein
Genistein
Cyclopamine
TAS102
Resveratrol
Olaparib
MK5108
ICG001
Buparlisib
Afatinib
SAHA
Trametinib
Regorafenib
5Fu
Belinostat
AUC
4
3
2
1
SNU-2414B
SNU-2414A
SNU-2404B
SNU-2404A
SNU-2335D
SNU-2335A

(B)

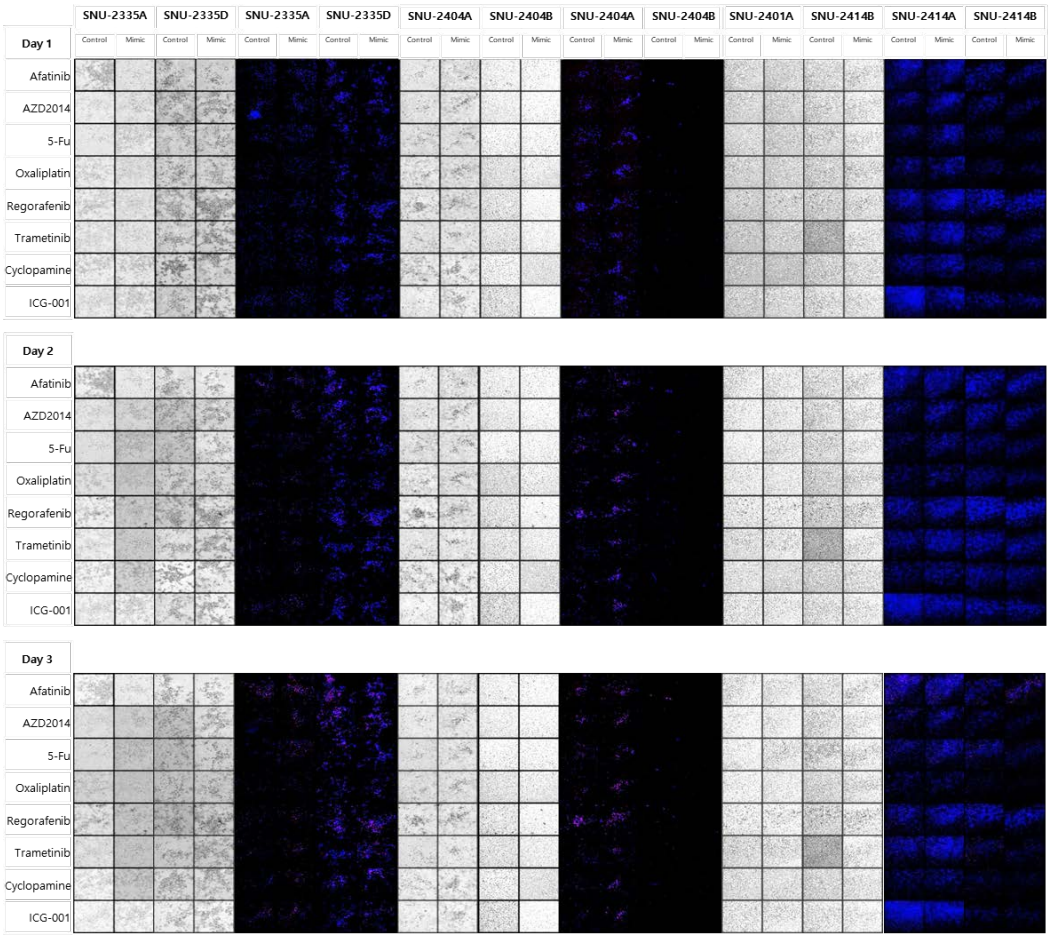
SNU-2335A
SNU-2335D
SNU-2335A
SNU-2335D
SNU-2404A
SNU-2404B
SNU-2404A
SNU-2404B
SNU-2401A
SNU-2414B
SNU-2414A
SNU-2414B
Control
Mimic
Day 1
Day 2
Day 3
Afatinib
AZD2014
5-Fu
Oxaliplatin
Regorafenib
Trametinib
Cyclopamine
ICG-001

(C)

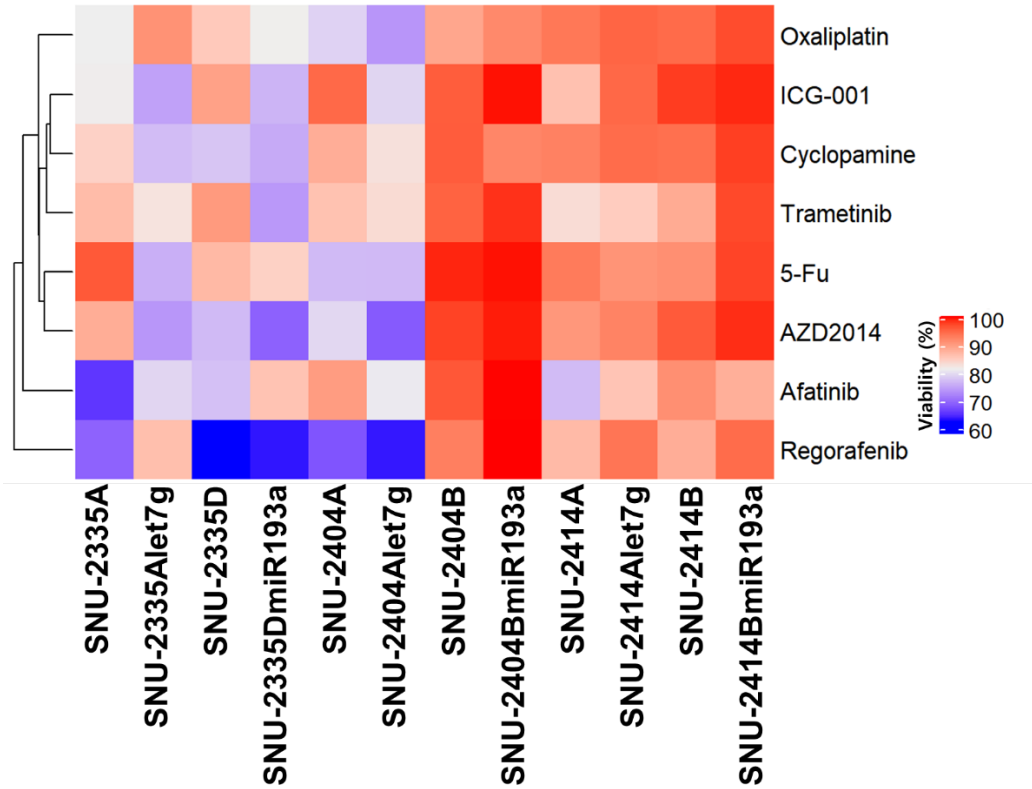
Oxaliplatin
ICG-001
Cyclopamine
Trametinib
5-Fu
AZD2014
Afatinib
Regorafenib
Viability (%)
100
90
80
70
60
SNU-2335A
SNU-2335Alet7g
SNU-2335D
SNU-2335DmiR193a
SNU-2404A
SNU-2404Alet7g
SNU-2404B
SNU-2404BmiR193a
SNU-2414A
SNU-2414Alet7g
SNU-2414B
SNU-2414BmiR193a

Figure 4. Multiple drug responsiveness in primary CRC and paired PTM

Cells were tested for drug sensitivity using a total of 24 FDA-approved anticancer drugs. The concentrations of anticancer agents are mentioned in the materials and methods section. (A) 24 drugs sensitivity of each cell line was compared through AUC value. (B) Cell viability of confocal microscopic image was observed for 72 h after selected 8 drugs treatment. Blue: Hoechst33342, Red: Propidium Iodide (PI). (C) Percentage of cell viability was performed by heatmap.

Multiple markers of colorectal cancer progression as exosomal miR-193a and exosomal let-7g

To identify exosomal miRNAs as colorectal cancer markers, the expression of exosomal miR-193a and exosomal let-7g was confirmed by using the exosomes in the plasma of colorectal cancer patients. Among the 69 patients having colorectal cancer, those who were 80 years old were the most common, and their staging was most frequently AJCC (*American Joint Committee on Cancer*) stage Ⅱ (table3).

As the AJCC staging progressed to a high grade, exosomal miR-193a expression decreased significantly in all stages as compared to stage Ⅰ, and exosomal let-7g significantly increased in all stages except in stage Ⅰ (Figure 5A). The recurrence group had less miR-193a expression than did the group not having recurrence and let-7g expression was significantly higher (Figure 5B). The expression of exosomal miR-193a and exosomal let-7g were identified, according to the concentration of carcinoembryonic antigen (CEA), and the expression of let-7g did not show a

significant difference at various concentration levels. On the other hand, the expression of miR-193a showed a significant decrease in the level of CEA (> 5 ng/mL) as compared to other concentration levels (Figure 5C). The expression of exosomal miR-193a was not different according to the presence or absence of lymphatic invasion, but the expression of let-7g was higher in the group with lymphatic invasion than in the group without lymphatic invasion (Figure 5D). The expression of exosomal miR-193a and exosomal let-7g, in accordance with the presence or absence of venous invasion, was the same as the expression pattern with recurrence. The group with venous invasion had a lower miR-193a expression and a higher level of let-7g than did the group without venous invasion (Figure 5E).

Table 3. Colorectal cancer patient profile

Colorectal cancer patient profile (Total *n* = 69)							
Sex	Male	44					
	Female	25					
Age	Total	<40	<50	<60	<70	<80	80≤
	39-84	1	4	22	16	23	3
Lymphatic invasion	Absence	55					
	Presence	14					
Venous invasion	Absence	52					
	Presence	17					
AJCC stage	Ⅰ	Ⅱ	Ⅲ	Ⅳ			
	6	29	26	8			

Figure 5

(A)

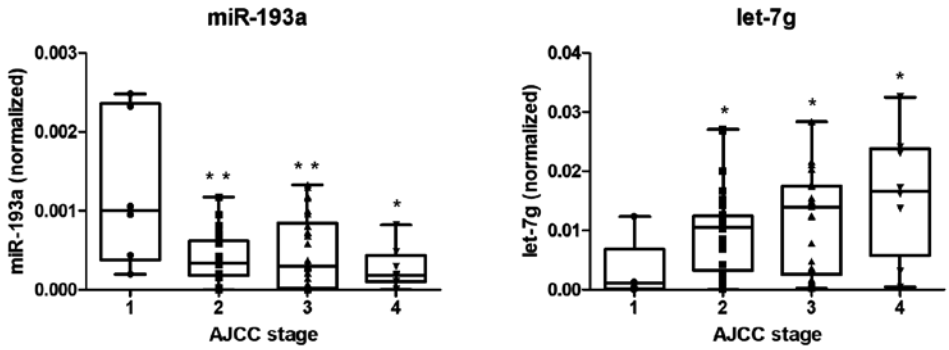
miR-193a
miR-193a (normalized)
0.003
0.002
0.001
0.000
1
2
3
4
AJCC stage
let-7g
let-7g (normalized)
0.04
0.03
0.02
0.01
0.00
1
2
3
4
AJCC stage

(B)

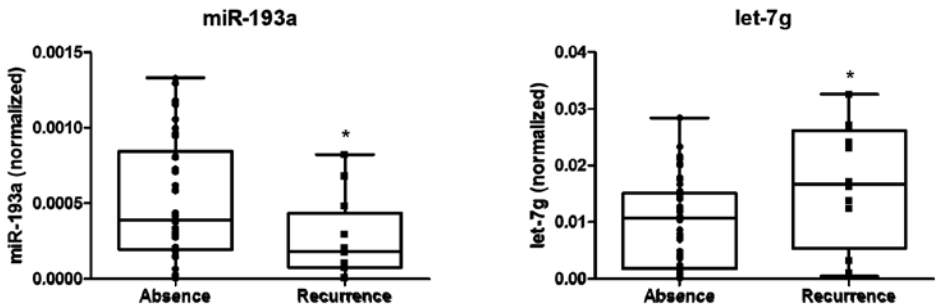
miR-193a
miR-193a (normalized)
0.0015
0.0010
0.0005
0.0000
Absence
Recurrence
let-7g
let-7g (normalized)
0.04
0.03
0.02
0.01
0.00
Absence
Recurrence

(C)

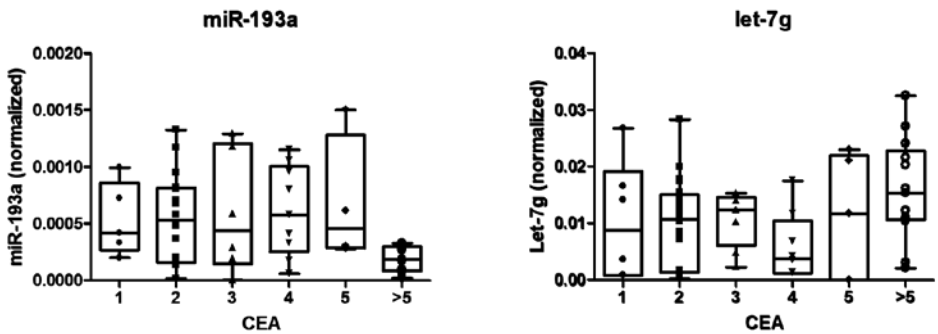
miR-193a
miR-193a (normalized)
0.0020
0.0015
0.0010
0.0005
0.0000
1
2
3
4
5
>5
CEA
let-7g
Let-7g (normalized)
0.04
0.03
0.02
0.01
0.00
1
2
3
4
5
>5
CEA

(D)

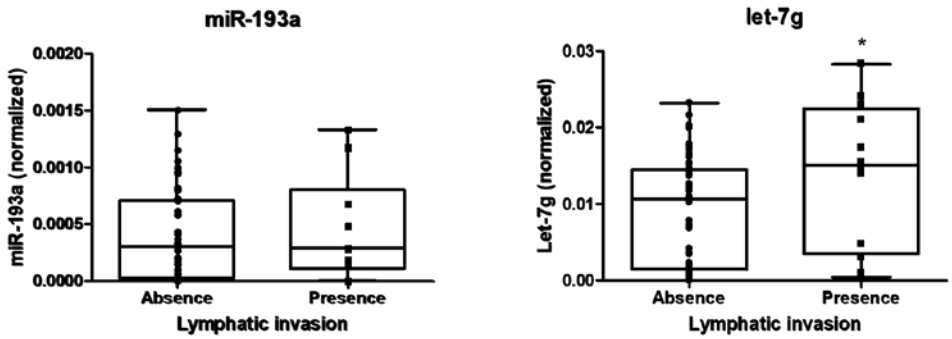
miR-193a
miR-193a (normalized)
0.0020
0.0015
0.0010
0.0005
0.0000
Absence
Presence
Lymphatic invasion
let-7g
Let-7g (normalized)
0.03
0.02
0.01
0.00
*
Absence
Presence
Lymphatic invasion

(E)

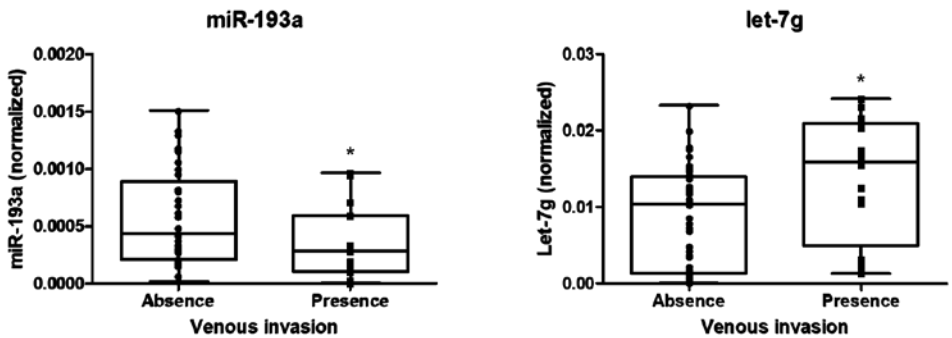
miR-193a
miR-193a (normalized)
0.0020
0.0015
0.0010
0.0005
0.0000
*
Absence
Presence
Venous invasion
let-7g
Let-7g (normalized)
0.03
0.02
0.01
0.00
*
Absence
Presence
Venous invasion

Figure 5. Correlation between clinical factors and exosomal miRNA expression

Expression of exosomal miR-193a and let-7g extracted from plasma of colorectal cancer patients was confirmed based on various clinical factors. Data is presented by 1-way ANOVA as compared to AJCC stage1 and CEA ≤ 1 group. Dunnett's test was used as a post-hoc analysis (A and C). Data is presented by t-test as compared to absence group (B, D and E). $*p < 0.05$ and $**p < 0.01$. (A) Cancer stage, (B) Recurrence, (C) CEA, (D) Lymphatic invasion, (E) Venous invasion

Clinical correlation of exosomal miR-193a and exosomal let-7g on colorectal cancer prognosis

Through cell line analysis, exosomal miR-193a was significantly lower in all types of metastatic cell lines than it was in primary colorectal cancer cell lines, and exosomal let-7g was higher in peritoneal metastatic cell lines than in primary colorectal cancer cell lines (Figure 2A-B).

Based on the results of the exosomal miRNA experiment derived from plasma, it was confirmed that the negative correlation between miR-193a and let-7g was significant (Figure 6A).

As described in the Materials and Methods section, the cutoff points of two exosomal miRNAs (miR-193a and let-7g) were respectively determined with the MaxStat R Package program in order to divide the high and low expression groups for two exosomal miRNAs. The group with a high expression of exosomal miR-193a had a greater patient survival rate than did the low expression group, whereas the group with a high exosomal let-7g expression had a lower survival rate than did the group with a low expression (Figure

6B-C). Based on the aforementioned results, there was a significant difference in survival rate between the miR-193a high and let-7g low group and the miR-193a low and let-7g high group (Figure 6D). Consequently, the lower the expression of exosomal miR-193a, the greater the expression of exosomal let-7g, and the patient prognosis was poorer.

Figure 6

(A)

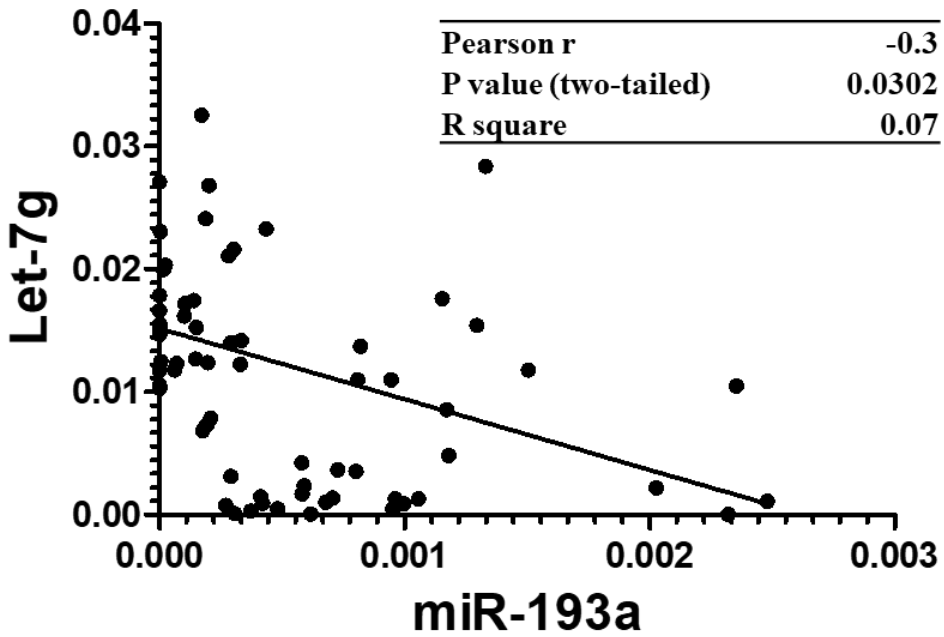
Pearson r -0.3
P value (two-tailed) 0.0302
R square 0.07
Let-7g
0.04
0.03
0.02
0.01
0.00
0.000
0.001
0.002
0.003
miR-193a

(B)

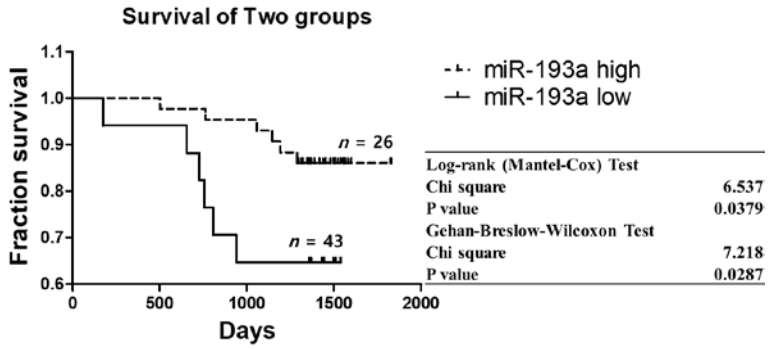
Survival of Two groups
Fraction survival
Days
n = 26
n = 43
miR-193a high
miR-193a low
Log-rank (Mantel-Cox) Test
Chi square 6.537
P value 0.0379
Gehan-Breslow-Wilcoxon Test
Chi square 7.218
P value 0.0287

(C)

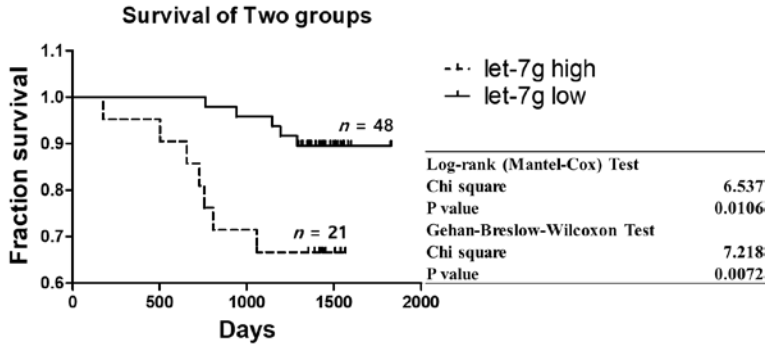
Survival of Two groups
Fraction survival
Days
n = 48
n = 21
let-7g high
let-7g low
Log-rank (Mantel-Cox) Test
Chi square 6.537
P value 0.0106
Gehan-Breslow-Wilcoxon Test
Chi square 7.218
P value 0.0072

(D)

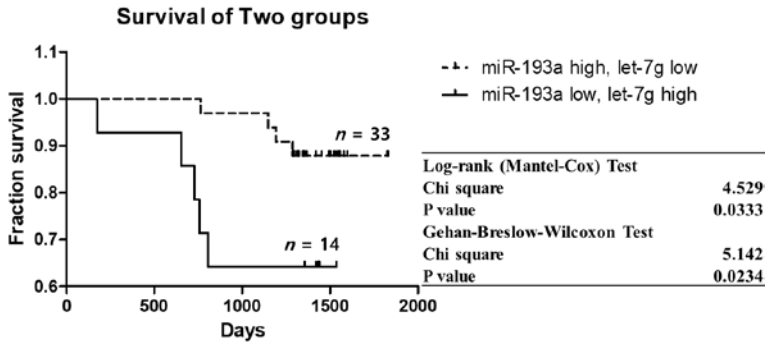
Survival of Two groups
Fraction survival
Days
n = 33
n = 14
miR-193a high, let-7g low
miR-193a low, let-7g high
Log-rank (Mantel-Cox) Test
Chi square 4.529
P value 0.0333
Gehan-Breslow-Wilcoxon Test
Chi square 5.142
P value 0.0234

Figure 6. Mutual and clinical correlation of exosomal miR-193a and let-7g expression

(A) Exosomal miR-193a and exosomal let-7g from the same patient have a significant negative correlation. Pearson r: -0.3, $p < 0.0302$. (B) Kaplan-meier plot according to high or low expression group of exosomal miR-193a. $p < 0.0379$; (C) Kaplan-meier plot according to high or low expression group of exosomal let-7g. (D) Kaplan-meier plot according to combined high or low expression group of exosomal miR-193a and let-7g. $p < 0.0333$. miR-193a cutoff point: 0.000193 and let-7g cutoff point: 0.0154. $p < 0.0106$.

DISCUSSION

Peritoneal metastasis of colorectal cancer is the third most common form of metastasis, but the prognosis of patients with colorectal metastasis is the worst (4). Peritoneal metastasis is divided into a synchronous type, a simultaneous type, and a metachronous type. These occur after colorectal cancer onset. Synchronous peritoneal metastasis occurs in about 4% to 13% of all colorectal cancer patients, and metachronous disease occurs in up to 19% of all patients (34). The peritoneum is a fertile location where metastasis develops largely because of its large surface area. The process of peritoneal metastasis is based upon the "tumor cell entrapment" phenomenon (35).

This process proceeds to shedding, binding, migration, and survival (at completion of peritoneal metastasis). In the shedding stage, primary colorectal cancer is able to penetrate many layers (including mucosa, submucosa, and serosa) and then to detached from the primary tumor (36). In addition, invasiveness, as well as cell growth, is also one of the abilities that cancer cells attached to

peritoneum must successfully survive in the migration stage (37).

There are no specific symptoms of peritoneal metastasis, and imaging modalities such as computed tomography (CT) and 18F-fluorodeoxyglucose Positron Emission Tomography/Computed Tomography (PET-CT) are used for the diagnosis of peritoneal metastasis. Most studies have found that CT scanning has limited sensitivity in detecting peritoneal nodules < 0.5 cm, with improved sensitivity to increased lesion size (38).

In this study, primary CRC and PTM derived from the same patient were established as cell lines (39). Unlike liver metastasis or lymph node metastasis, peritoneal metastasis has a unique mechanism of mesothelial metastasis that occurs at a close physical distance (40). Therefore, it is known that an exosome autocrine signaling system is generated (41-43), but a local environment may occur in which an autocrine signaling system cannot be formed. Because of the environmental differences, it is believed that increasing exosomal miRNAs, as well as decreasing miRNAs between the primary CRC-paired PTMs, can play a crucial role in colorectal peritoneal

metastasis.

Consequently, this study elucidated the importance of exosomal miRNA in CPM as well as its usefulness as a diagnostic marker for identifying the difference in expression of exosomal miRNA between CRC-PTM sets and revealing what role the protein targeted by exosomal miRNA plays in metastasis.

All three pairs of CRC-PTM cell lines were grown in adherent cell types except for SNU-2404B (Figure 1A). The TNM stages of the patients derived from these cell lines were SNU-2335A (T3N2M1), SNU-2335D (T3N2M1), SNU-2404A (T4bN2M1), SNU-2404B (T4bN2M1), SNU-2414A (T4bN2M1), and SNU-2414B (T4bN2M1), respectively (39).

In MDS results based upon miRNA microarray data (Figure 1C), three primary CRC groups (SNU-2335A, SNU-2404A and SNU-2414A) were concentrated at similar points, whereas PTM groups (SNU-2335D, SNU-2404B and SNU-2414B) were found to be scattered. It was found that PTM groups had different characteristics from the primary CRC group to which they belonged

in accordance with the MDS results. To manage the batch effect of the microarray, exosomal miRNA was extracted from a medium cultured with cells of the same passage and similar cell density, and microarray analysis was performed using the same panel at the same time. The TOP 5 miRNA list was classified according to the differences in the miRNA expressions between the CRC-PTM sets (table1). A DIANA-miRPath analysis was performed to understand the overall properties of a total of 16 miRNAs. Let-7g-5p (with fold change $\geq$ 2) and miR-193a-5p (with fold change $\leq$ 2) were selected through this analysis (Figure 1D-E). The genes targeted by let-7g and miR-193a were analyzed by using three target prediction programs (miRDB, miRWalk, and TargetScan). Subsequently, it was confirmed that let-7g targets were the *CDKN1A* and *TGFBR1*, and the miR-193a targets were the *MMP16* and the *ACVR1*.

The RNA expression of *MMP16* in all cell lines was higher in the peritoneal groups than in the primary CRC group. However, protein expression was the same in the peritoneal metastatic set except for

the SW480-620 set and the KC12C-1214 set (Figure 2C). Since the *MMP16* is involved in a process of epithelial-mesenchymal transition (EMT) such as cell invasion and intravasation (44,45), it was necessary to confirm the protein expression of E-cadherin used as a marker of EMT (46). Transfection of miR-193a mimic was induced to increase E-cadherin in SNU-2335D and SNU-2404B. The results of reduced MMP16 and increased E-cadherin by miR-193a mimic confirmed that miR-193a mimic may possibly be involved in the EMT of CPM. Based on the results of exosomal miRNA microarray analysis, let-7g, which shows more expression in the peritoneal metastatic cell line group, was expected to induce decreased E-cadherin expression and increased snail expression as opposed to miR-193a. But in fact, there was no obvious aspect except for SNU-2335A (Figure 2D). This suggests that *CDKN1A* and *TGFBR1*, which were selected as let-7g target genes, are involved in cell proliferation or cell growth, so that this is not likely to have a significant effect on the expression of E-cadherin and snail, known to be EMT markers.

The cell invasiveness was identified by transfection of miRNA mimic, and it was confirmed that the transfection of miR-193a mimic into the peritoneal metastatic group significantly reduced the invasiveness as compared to the control group. The chemotaxis was induced by using an FBS-free medium and a medium with FBS, and the invasiveness was generated in a right-to-left direction. The treatment of miR-193a mimic to the peritoneal metastatic cell line and the let-7g to the primary colorectal cancer cell line were designed to mimic the *in vivo* conditions as much as possible, based on the miRNA analysis results. (Figure 3A-C). A crucial factor in cancer metastasis is not only cell invasiveness, but also cell proliferation. Therefore, Ki-67 immunofluorescence and cell cycle assay were performed to confirm the effect of the exosomal miRNA mimic on cell proliferation. The expression of Ki-67 on the let-7g treatment group was higher than that of control group in SNU-2335A. On the other hand, the effect of miR-193a mimic on the expression of Ki-67 was not significant, whereas the effect of let-7g mimic showed a difference as compared to the control group (Figure 3D-E). Because of the spheroid-like form of the SNU-

2404A and SNU-2414A, permeabilization and staining of cells inside the colony were not well performed, and they were not suitable for immunofluorescence experiments.

These results suggest that *CDKN1A* targeted by let-7g is directly involved in the cell cycle, and *MMP16* targeted by miR-193a is directly involved in cell invasiveness rather than cell proliferation.

Cell viability to a total of 24 drugs was confirmed in SNU-2335 set, SNU-2404 set and SNU-2414 set (Figure 4A), and a total of 8 drugs were classified into high AUC group (AZD2014 and Oxaliplatin), intermediate AUC group (Cyclopamine, ICG-001 and Afatinib) and low AUC group (Trametinib, Regorafenib and 5-FU) according to AUC value. Afatinib, a second-generation EGFR-TKI, is known as an irreversible inhibitor of ERBB2 and EGFR (47), and AZD2014 is known as an inhibitor of mTOR (48). *CDKN1A* and *TGFBR1* were targeted by let-7g (table2). This showed a higher expression in the peritoneal metastatic cell line than in the primary CRC cell line and played a role in inducing cell cycle arrest (49). It is speculated that *CDKN1A* inactivated by let-7g was relatively

more damaged by afatinib and AZD2014, which mainly inhibits cell proliferation and survival in peritoneal metastatic cell lines, where cell proliferation is more active. Based on a heatmap showing cell viability, it was confirmed that the cell viability of the let-7g treatment group was lower than that of control group in SNU-2335A and SNU-2404A (Figure 4B-C). The image analysis of live/dead cells through the Hoechst33342 and PI staining was relatively inaccurate in the SNU-2404B, SNU-2414A, and SNU-2414B. The SNU-2404B was in the form of a floating cell, so it was difficult to focus the confocal microscope to confirm PI staining. Both SNU-2414A and SNU-2414B characteristically grow into a dome shape after gathering in the middle of a well. So, it is believed that the drugs and PI staining solution could not effectively penetrate into the dome shape.

Based on cell line studies, the results obtained from exosomal miRNA extracted from the plasma of colorectal cancer patients show that the more severe the colorectal cancer becomes, the lower the miR-193a expression and the higher the let-7g expression are.

The expression of miR-193a and let-7g was confirmed through various factors, including colorectal cancer staging, recurrence, lymphatic invasion, and venous invasion, showing significant differences as compared to the control group (Figure 5A-E). These factors were expected to have a close correlation to the cancer prognosis. Subsequently, we investigated the five-year survival rate of patients and confirmed that miR-193a and let-7g were classified as a high expression group and a low expression group and that they showed a significant difference (Figure 6B-C). It was confirmed that the decrease in the expression of miR-193a and the increase in the expression of let-7g significantly decreased the patient's survival rate, respectively. Additionally, the combinational effect of miR-193a and let-7g induced a significant decrease in patient survival rate compared to the control group (Figure 6D), and these results support the fact that there is a negative correlation (Figure 6A, Pearson R=-0.3) as cancer progression progresses.

The clinical studies of exosomal miR-193a and let-7g were more general in disease progression and patient prognosis, not strictly in

peritoneal metastatic cases. Although changes in miR-193a and let-7g expressions were consequently significant, the causal relationship between the possibility of peritoneal metastasis and the expression of the two miRNAs is not clear. Therefore, further study is necessary to obtain more abundant cases and to standardize the expression thresholds of miR-193a and let-7g according to the presence or absence of peritoneal metastasis in the same tumor stage.

Because the amount of exosomal miRNA is small, it is important to set a cutoff point to distinguish between high expression and low expression. Although the half-life of miRNAs preserved in the exosomes are relatively long (50,51), the amount and proportion of exosomal miRNAs extracted from a fresh plasma sample may possibly be different from those extracted from a plasma stored for five years. Therefore, the amount of exosomal miR-193a and let-7g in the fresh plasma sample might be different, and the cutoff point will also need to be changed.

Despite the limitations of this study, if further studies on the

expression of exosomal miR-193a and let-7g are conducted in fresh plasma samples, the cutoff points of the two miRNAs will be clearly elucidated. Furthermore, exosomal miR-193a and let-7g might be used as markers to predict the progression and prognosis of colorectal cancer.

Taken together, the results of our research show that primary CRC and paired PTM cancers have different characteristics in the expression of exosomal miRNA, and among them, miR-193a and let-7g, which show significant difference, are validated. In PTM cancer, both the activation of *MMP16* and the inhibition of *CDKN1A* induced an acceleration of cancer invasiveness because of a decrease in miR-193a and an increase in let-7g. The reduction of exosomal miR-193a and the increase of exosomal let-7g extracted from plasma of colorectal cancer patients became more significant following poor prognosis indicators, including cancer staging, recurrence, venous invasion, and lymphatic invasion. Exosomal miR-193a and let-7g, which express opposite to cancer progressions, have a negative correlation. Both a low expression of

miR-193a and a high expression of let-7g significantly decrease the patient survival rates. Consequently, exosomal miR-193a and let-7g play a crucial role in cancer progression and clinically have great potential as cancer prognostic markers.

REFERENCES

1. Araghi M, Soerjomataram I, Jenkins M, Brierley J, Morris E, Bray F, *et al.* Global trends in colorectal cancer mortality: projections to the year 2035. *Int J Cancer* 2019;**144**(12):2992-3000 doi 10.1002/ijc.32055.
2. Jayne DG, Fook S, Loi C, Seow-Choen F. Peritoneal carcinomatosis from colorectal cancer. *Br J Surg* 2002;**89**(12):1545-50 doi 10.1046/j.1365-2168.2002.02274.x.
3. Lemmens VE, Klaver YL, Verwaal VJ, Rutten HJ, Coebergh JW, de Hingh IH. Predictors and survival of synchronous peritoneal carcinomatosis of colorectal origin: a population-based study. *Int J Cancer* 2011;**128**(11):2717-25 doi 10.1002/ijc.25596.
4. Segelman J, Granath F, Holm T, Machado M, Mahteme H, Martling A. Incidence, prevalence and risk factors for peritoneal carcinomatosis from colorectal cancer. *Br J Surg* 2012;**99**(5):699-705 doi 10.1002/bjs.8679.

5. Franko J, Shi Q, Goldman CD, Pockaj BA, Nelson GD, Goldberg RM, *et al.* Treatment of colorectal peritoneal carcinomatosis with systemic chemotherapy: a pooled analysis of north central cancer treatment group phase III trials N9741 and N9841. *Journal of clinical oncology : official journal of the American Society of Clinical Oncology* 2012;**30**(3):263-7 doi 10.1200/jco.2011.37.1039.

6. Ketcham AS, Hoye RC, Pilch YH, Morton DL. Delayed intestinal obstruction following treatment for cancer. *Cancer* 1970;**25**(2):406-10 doi 10.1002/1097-0142(197002)25:2<406::Aid-cncr2820250219>3.0.Co;2-4.

7. Verwaal VJ, van Ruth S, de Bree E, van Sloothen GW, van Tinteren H, Boot H, *et al.* Randomized trial of cytoreduction and hyperthermic intraperitoneal chemotherapy versus systemic chemotherapy and palliative surgery in patients with peritoneal carcinomatosis of colorectal cancer. *Journal of clinical oncology : official journal of the American Society of Clinical Oncology* 2003;**21**(20):3737-43 doi 10.1200/jco.2003.04.187.

8. Pelz JO, Chua TC, Esquivel J, Stojadinovic A, Doerfer J, Morris DL, *et al.* Evaluation of best supportive care and systemic chemotherapy as treatment stratified according to the retrospective peritoneal surface disease severity score (PSDSS) for peritoneal carcinomatosis of colorectal origin. *BMC Cancer* 2010;**10**:689 doi 10.1186/1471-2407-10-689.

9. Franko J, Shi Q, Meyers JP, Maughan TS, Adams RA, Seymour MT, *et al.* Prognosis of patients with peritoneal metastatic colorectal cancer given systemic therapy: an analysis of individual patient data from prospective randomised trials from the Analysis and Research in Cancers of the Digestive System (ARCAD) database. *Lancet Oncol* 2016;**17**(12):1709-19 doi 10.1016/s1470-2045(16)30500-9.

10. Cravioto-Villanueva A, Cavazos M, Luna-Perez P, Martinez-Gomez H, Ramirez ML, Solorzano J, *et al.* Cytoreductive surgery with hyperthermic intraperitoneal chemotherapy (HIPEC) delivered via a modified perfusion system for peritoneal carcinomatosis of colorectal origin. *Surg Today*

2016;**46**(8):979-84 doi 10.1007/s00595-016-1335-3.

11. Spiliotis J, Kalles V, Kyriazanos I, Terra A, Prodromidou A, Raptis A, *et al.* CRS and HIPEC in patients with peritoneal metastasis secondary to colorectal cancer: The small-bowel PCI score as a predictor of survival. *Pleura Peritoneum* 2019;**4**(4):20190018 doi 10.1515/pp-2019-0018.
12. Klaver YL, Simkens LH, Lemmens VE, Koopman M, Teerenstra S, Bleichrodt RP, *et al.* Outcomes of colorectal cancer patients with peritoneal carcinomatosis treated with chemotherapy with and without targeted therapy. *Eur J Surg Oncol* 2012;**38**(7):617-23 doi 10.1016/j.ejso.2012.03.008.
13. Elias D, Lefevre JH, Chevalier J, Brouquet A, Marchal F, Classe JM, *et al.* Complete cytoreductive surgery plus intraperitoneal chemohyperthermia with oxaliplatin for peritoneal carcinomatosis of colorectal origin. *Journal of clinical oncology : official journal of the American Society of Clinical Oncology* 2009;**27**(5):681-5 doi 10.1200/jco.2008.19.7160.
14. Klaver CE, Musters GD, Bemelman WA, Punt CJ, Verwaal VJ,

Dijkgraaf MG, *et al.* Adjuvant hyperthermic intraperitoneal chemotherapy (HIPEC) in patients with colon cancer at high risk of peritoneal carcinomatosis; the COLOPEC randomized multicentre trial. *BMC Cancer* 2015;**15**:428 doi 10.1186/s12885-015-1430-7.

15. Shida D, Yoshida T, Tanabe T, Tsukamoto S, Ochiai H, Kanemitsu Y. Prognostic Impact of R0 Resection and Targeted Therapy for Colorectal Cancer with Synchronous Peritoneal Metastasis. *Ann Surg Oncol* 2018;**25**(6):1646-53 doi 10.1245/s10434-018-6436-3.

16. Verwaal VJ, Bruin S, Boot H, van Slooten G, van Tinteren H. 8-year follow-up of randomized trial: cytoreduction and hyperthermic intraperitoneal chemotherapy versus systemic chemotherapy in patients with peritoneal carcinomatosis of colorectal cancer. *Ann Surg Oncol* 2008;**15**(9):2426-32 doi 10.1245/s10434-008-9966-2.

17. Norcic G. Liquid Biopsy in Colorectal Cancer-Current Status and Potential Clinical Applications. *Micromachines (Basel)* 2018;**9**(6):300 doi 10.3390/mi9060300.

18. Jacobson RA, Munding E, Hayden DM, Levy M, Kuzel TM, Pappas SG, *et al.* Evolving Clinical Utility of Liquid Biopsy in Gastrointestinal Cancers. *Cancers (Basel)* 2019;**11**(8):1164 doi 10.3390/cancers11081164.

19. De Rubis G, Rajeev Krishnan S, Bebawy M. Liquid Biopsies in Cancer Diagnosis, Monitoring, and Prognosis. *Trends in Pharmacological Sciences* 2019;**40**(3):172-86 doi 10.1016/j.tips.2019.01.006.

20. Bracci L, Lozupone F, Parolini I. The role of exosomes in colorectal cancer disease progression and response to therapy. *Cytokine & Growth Factor Reviews* 2020;**51**:84-91 doi https://doi.org/10.1016/j.cytogfr.2019.12.004.

21. Zhou J, Li X-L, Chen Z-R, Chng W-J. Tumor-derived exosomes in colorectal cancer progression and their clinical applications. *Oncotarget* 2017;**8**(59):100781-90 doi 10.18632/oncotarget.20117.

22. Xiao Y, Zhong J, Zhong B, Huang J, Jiang L, Jiang Y, *et al.* Exosomes as potential sources of biomarkers in colorectal cancer. *Cancer letters* 2020;**476**:13-22 doi

https://doi.org/10.1016/j.canlet.2020.01.033.

23. Matsumura T, Sugimachi K, Iinuma H, Takahashi Y, Kurashige J, Sawada G, *et al.* Exosomal microRNA in serum is a novel biomarker of recurrence in human colorectal cancer. *British journal of cancer* 2015;**113**(2):275-81 doi 10.1038/bjc.2015.201.

24. Silva J, García V, Rodríguez M, Compte M, Cisneros E, Veguillas P, *et al.* Analysis of exosome release and its prognostic value in human colorectal cancer. *Genes, chromosomes & cancer* 2012;**51**:409-18 doi 10.1002/gcc.21926.

25. Wu M, Wang G, Hu W, Yao Y, Yu X-F. Emerging roles and therapeutic value of exosomes in cancer metastasis. *Molecular Cancer* 2019;**18**(1):53 doi 10.1186/s12943-019-0964-8.

26. Keller S, Sanderson MP, Stoeck A, Altevogt P. Exosomes: from biogenesis and secretion to biological function. *Immunol Lett* 2006;**107**(2):102-8 doi 10.1016/j.imlet.2006.09.005.

27. Tsukamoto M, Iinuma H, Yagi T, Matsuda K, Hashiguchi Y. Circulating Exosomal MicroRNA-21 as a Biomarker in Each Tumor Stage of Colorectal Cancer. *Oncology* 2017;**92**(6):360-70 doi 10.1159/000463387.

28. Tang YT, Huang YY, Li JH, Qin SH, Xu Y, An TX*, et al.* Alterations in exosomal miRNA profile upon epithelial-mesenchymal transition in human lung cancer cell lines. *BMC Genomics* 2018;**19**(1):802 doi 10.1186/s12864-018-5143-6.

29. Wang H, Wei H, Wang J, Li L, Chen A, Li Z. MicroRNA-181d-5p-Containing Exosomes Derived from CAFs Promote EMT by Regulating CDX2/HOXA5 in Breast Cancer. *Molecular Therapy - Nucleic Acids* 2020;**19**:654-67 doi 10.1016/j.omtn.2019.11.024.

30. Grady WM, Tewari M. The next thing in prognostic molecular markers: microRNA signatures of cancer. *Gut* 2010;**59**(6):706-8 doi 10.1136/gut.2009.200022.

31. Pan C, Stevic I, Muller V, Ni Q, Oliveira-Ferrer L, Pantel K*, et al.* Exosomal microRNAs as tumor markers in epithelial

ovarian cancer. *Mol Oncol* 2018;**12**(11):1935-48 doi 10.1002/1878-0261.12371.

32. Kim S-C, Kim H-S, Kim JH, Jeong N, Shin Y-K, Kim MJ*, et al.* Establishment and characterization of 18 human colorectal cancer cell lines. *Scientific Reports* 2020;**10**(1):6801 doi 10.1038/s41598-020-63812-z.

33. Lässer C, Eldh M, Lötvall J. Isolation and characterization of RNA-containing exosomes. *J Vis Exp* 2012(59):e3037-e doi 10.3791/3037.

34. van Gestel YR, Thomassen I, Lemmens VE, Pruijt JF, van Herk-Sukel MP, Rutten HJ*, et al.* Metachronous peritoneal carcinomatosis after curative treatment of colorectal cancer. *Eur J Surg Oncol* 2014;**40**(8):963-9 doi 10.1016/j.ejso.2013.10.001.

35. Sugarbaker PH. Cytoreductive surgery and hyperthermic intraperitoneal chemotherapy in the management of gastrointestinal cancers with peritoneal metastases: Progress toward a new standard of care. *Cancer Treat Rev*

2016;48:42-9 doi 10.1016/j.ctrv.2016.06.007.

36. Ceelen WP, Bracke ME. Peritoneal minimal residual disease in colorectal cancer: mechanisms, prevention, and treatment. *Lancet Oncol* 2009;10(1):72-9 doi 10.1016/s1470-2045(08)70335-8.

37. Narasimhan V, Ooi G, Michael M, Ramsay R, Lynch C, Heriot A. Colorectal peritoneal metastases: pathogenesis, diagnosis and treatment options - an evidence-based update. *ANZ J Surg* 2020 doi 10.1111/ans.15796.

38. Koh JL, Yan TD, Glenn D, Morris DL. Evaluation of preoperative computed tomography in estimating peritoneal cancer index in colorectal peritoneal carcinomatosis. *Ann Surg Oncol* 2009;16(2):327-33 doi 10.1245/s10434-008-0234-2.

39. Kim SC, Hong CW, Jang SG, Kim YA, Yoo BC, Shin YK, *et al.* Establishment and Characterization of Paired Primary and Peritoneal Seeding Human Colorectal Cancer Cell Lines: Identification of Genes That Mediate Metastatic Potential. *Transl Oncol* 2018;11(5):1232-43 doi

10.1016/j.tranon.2018.07.014.

40. Lemoine L, Sugarbaker P, Van der Speeten K. Pathophysiology of colorectal peritoneal carcinomatosis: Role of the peritoneum. *World J Gastroenterol* 2016;**22**(34):7692-707 doi 10.3748/wjg.v22.i34.7692.

41. Ziober BL, Willson JK, Hymphrey LE, Childress-Fields K, Brattain MG. Autocrine transforming growth factor-alpha is associated with progression of transformed properties in human colon cancer cells. *J Biol Chem* 1993;**268**(1):691-8.

42. Warn R, Harvey P, Warn A, Foley-Comer A, Heldin P, Versnel M, *et al.* HGF/SF induces mesothelial cell migration and proliferation by autocrine and paracrine pathways. *Exp Cell Res* 2001;**267**(2):258-66 doi 10.1006/excr.2001.5240.

43. Bhowmick NA, Neilson EG, Moses HL. Stromal fibroblasts in cancer initiation and progression. *Nature* 2004;**432**(7015):332-7 doi 10.1038/nature03096.

44. Cao L, Chen C, Zhu H, Gu X, Deng D, Tian X, *et al.* MMP16 is a marker of poor prognosis in gastric cancer promoting proliferation and invasion. *Oncotarget* 2016;**7**(32):51865-74

doi 10.18632/oncotarget.10177.

45. Wu S, Ma C, Shan S, Zhou L, Li W. High expression of matrix metalloproteinases 16 is associated with the aggressive malignant behavior and poor survival outcome in colorectal carcinoma. *Scientific Reports* 2017;**7**(1):46531 doi 10.1038/srep46531.

46. Tatti O, Gucciardo E, Pekkonen P, Holopainen T, Louhimo R, Repo P, *et al.* MMP16 Mediates a Proteolytic Switch to Promote Cell-Cell Adhesion, Collagen Alignment, and Lymphatic Invasion in Melanoma. *Cancer research* 2015;**75**(10):2083-94 doi 10.1158/0008-5472.Can-14-1923.

47. D'Arcangelo M, Hirsch FR. Clinical and comparative utility of afatinib in non-small cell lung cancer. *Biologics* 2014;**8**:183-92 doi 10.2147/btt.S40567.

48. Langdon S, Hughes A, Taylor MA, Kuczynski EA, Mele DA, Delpuech O, *et al.* Combination of dual mTORC1/2 inhibition and immune-checkpoint blockade potentiates anti-tumour immunity. *Oncoimmunology* 2018;**7**(8):e1458810-e doi

10.1080/2162402X.2018.1458810.

49. Asada M, Yamada T, Ichijo H, Delia D, Miyazono K, Fukumuro K, *et al.* Apoptosis inhibitory activity of cytoplasmic p21(Cip1/WAF1) in monocytic differentiation. *Embo j* 1999;**18**(5):1223-34 doi 10.1093/emboj/18.5.1223.

50. Marzi MJ, Ghini F, Cerruti B, de Pretis S, Bonetti P, Giacomelli C, *et al.* Degradation dynamics of microRNAs revealed by a novel pulse-chase approach. *Genome Res* 2016;**26**(4):554-65 doi 10.1101/gr.198788.115.

51. Göran Ronquist K. Extracellular vesicles and energy metabolism. *Clin Chim Acta* 2019;**488**:116-21 doi 10.1016/j.cca.2018.10.044.

국문 초록

대장암은 모든 암 질환을 통틀어 세계에서 세 번째로 많은 발병률을 보이고 있으며, 2035년까지 240만명 가량이 발생할 것으로 내다보고 있다. 대장암이 전이 및 재발이 되는 곳 중의 하나인 복막은 다수의 신경, 혈관과 림프관들이 연결되어 있다. 대장암이 재발하거나 전이가 일어나는 곳 중에서 두 번째로 빈번한 곳이 복막으로 알려져 있다. 대장암의 복막 전이는 다른 장기로의 전이에서 흔히 보이는 lymphatic metastasis와 복막 전이에서만 독특하게 나타나는 mesothelial metastasis로 나누어진다. 복막 전이가 일어난 대장암 세포들은 크기가 매우 작고 납작한 형태로 퍼져서 자라는 특징이 있다. 복막 전이 초기에는 computed tomography (CT)나 positron emission tomography (PET)등 시각적 진단기법으로는 파악하기가 매우 까다롭고 힘들어서 대장암이 말기까지 진행된 뒤 발견되는 경우가 많다. 최근에는 Hyperthermic intraperitoneal chemotherapy (HIPEC) 과 second-look surgery를 통한 치료법이 시행되고 있으나, 예후가 좋지 않을뿐더러 복막 전이 암의 경우 대장암의 systemic therapy에도 상대적으로 강한 내성을 보이는 경향이 있다. 이러한 위험에도 불구하고 대장암이 다른 장기로 전이가 된 경우에 대한 연구는 활발히 이루어지고

있는 반면, 원발 대장암의 복막 전이에 대한 유전자적 분석에 대한 연구는 상대적으로 부족한 편이다. 대장암과 관련된 최신 연구들의 동향은 환자 혈액의 액상 생체 검사를 통해 항암제 내성, 재발 및 전이의 가능성에 대해 비교적 빠른 시간에 파악하고 대응하고자 하는 방향으로 이루어지고 있다. 액상 생체 검사의 표적 중 하나로 exosome이 있는데 exosome은 세포가 분비하는 extracellular vesicle 중 지름이 30 ~ 150 μm 사이의 vesicle로 알려져 있으며, 세포 내의 다양한 핵산 물질과 단백질을 함유하고 있다. 또한 exosome은 다양한 경로를 통해 비교적 쉽게 다른 세포 내로 흡수가 가능하여 한 세포가 분비한 exosome 내 함유 성분들이 다른 세포로 흡수되어 신호 전달 체계에 영향을 주는 것으로 알려져 있다. Exosome 내의 물질 중에서 microRNA는 전체의 약 1 ~ 5%로 매우 적은 비중을 차지하는 반면, RNA를 직접적으로 억제할 수 있는 기능을 가지고 있어서, 세포의 신호 전달 체계에 중요한 역할을 수행한다고 알려져 있다. 실제로 다른 암 종에서 exosomal microRNA가 암 세포 특성 변화 (epithelial–mesenchymal transition) 및 암 미세환경에 중요한 역할을 수행한다는 연구결과들이 발표되었다. 따라서 exosomal microRNA가 독특한 전이 기작을 가지고 있는 대장암의 복막 전이 과정에서 암 세포의 특성변화와 암 미세환경에 중요한 역할을 수행할 것으로 기대했으며, 따

라서 동일 환자 유래의 원발 대장암과 복막 전이 암 세포주에서 유의적인 차이를 보이는 exosomal miRNA들을 발굴하여 대장암의 복막 전이 과정에서의 명확한 역할을 밝히고 나아가서 진단 및 예후를 확인할 수 있는 지표로써 임상적인 의미를 가질 가능성을 확인하고자 하는 목표로 연구를 진행하게 되었다. 동일 환자 유래 원발 대장암 세포주와 복막 전이암 세포주에서 추출한 exosomal miRNA를 microarray 기법을 통해 유의적인 차이를 보이는 miR-193a와 let-7g를 선별했다. 이들은 원발 대장암에 비해 복막 전이암에서 miR-193a의 발현은 감소했고, let-7g의 발현은 증가했다. Exosomal miR-193a와 let-7g의 표적 유전자로 각각 MMP16과 CDKN1A가 선별되었으며, qRT-PCR 기법을 통해 이들 miRNA들이 유의적으로 MMP16과 CDKN1A의 RNA 발현을 억제한다는 것을 확인했다. 생리학적인 기능을 파악하기 위해 두 miRNA들의 유사체를 세포주에 주입했으며, exosomal miR-193a에 의해 암세포의 침투능과 증식은 감소했고, exosomal let-7g에 의해 암세포의 침투능과 증식이 증가했다. 이 결과들을 바탕으로 실제 대장암 환자의 혈액에서 추출한 exosomal miRNA들로 진단 및 예후와 관련된 요소들에 따라 miRNA의 발현양을 확인했다. Exosomal miR-193a의 발현은 대장암 진행단계 높아짐에 따라 감소했으며, exosomal let-7g의 발현은 증가했다. 또한 exosomal miR-193a의 발현이 상대

적으로 낮은 집단은 높은 집단에 비해 생존률이 유의적으로 떨어졌으며, exosomal let-7g의 발현이 상대적으로 높은 집단은 낮은 집단에 비해 생존률이 역시 떨어졌다. 결론적으로 대장암의 exosomal miR-193a의 발현 감소와 let-7g의 발현 증가는 세포침투능과 세포증식을 유발하여 복막 전이를 가속화 시켰고, 실제 대장암 환자의 생존률 또한 감소시켰다. 따라서 혈액을 통해 추출 가능한 exosomal miR-193a와 let-7g는 임상적으로 진단 및 예후를 판단하는 지표로써의 높은 가능성을 확인할 수 있었다.

주요어: 대장암, 복막전이, 엑소좀, miR-193a, let-7g

학 번: 2014-30668